Cell Reports

Report

N^6-Methyladenosine Inhibits Local Ribonucleolytic Cleavage to Stabilize mRNAs in *Arabidopsis*

Graphical Abstract

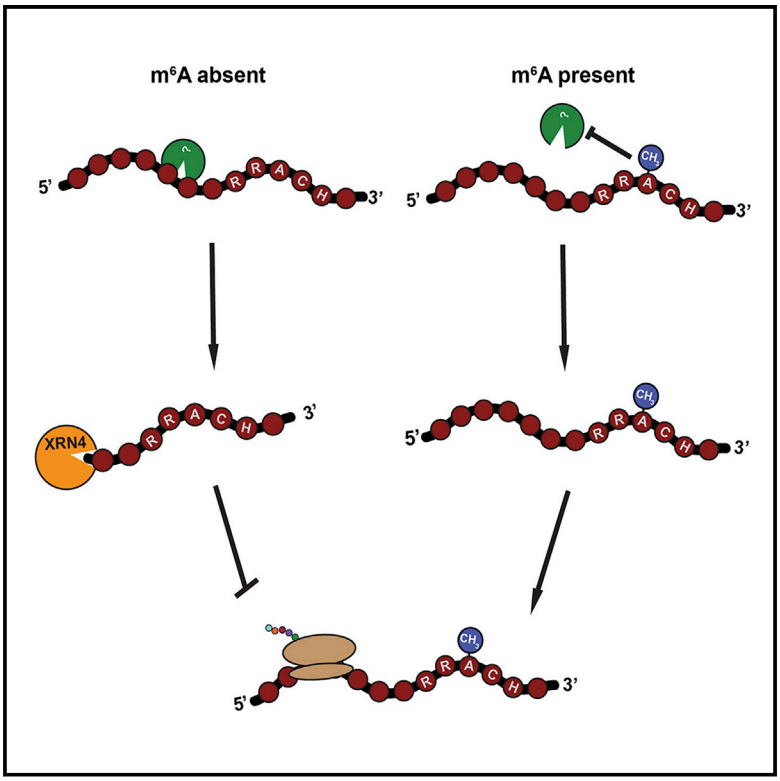

Authors

Stephen J. Anderson, Marianne C. Kramer, Sager J. Gosai, ..., Rupert G. Fray, Eric Lyons, Brian D. Gregory

Correspondence

bdgregor@sas.upenn.edu

In Brief

N^6-methyladenosine (m^6A) is the most prevalent internal covalent mRNA modification and is essential for proper function and regulation of the transcriptome. Using multiple transcriptome-wide approaches, Anderson et al. reveal that, in plant somatic tissue, m^6A stabilizes transcripts by inhibiting ribonucleolytic cleavage directly upstream of these modification sites.

Highlights

- m^6A sites are highly maintained at different *Arabidopsis* developmental stages
- Many m^6A sites stabilize *Arabidopsis* adult leaf transcripts
- m^6A stabilizes mRNAs through inhibition of local ribonucleolytic cleavage
- Dynamic, stress-specific m^6A sites stabilize stress response protein transcripts

Anderson et al., 2018, Cell Reports *25*, 1–12
October 30, 2018
https://doi.org/10.1016/j.celrep.2018.10.020

CellPress

Please cite this article in press as: Anderson et al., N6-Methyladenosine Inhibits Local Ribonucleolytic Cleavage to Stabilize mRNAs in *Arabidopsis*, Cell Reports (2018), https://doi.org/10.1016/j.celrep.2018.10.020

Cell Reports
Report

N^6-Methyladenosine Inhibits Local Ribonucleolytic Cleavage to Stabilize mRNAs in *Arabidopsis*

Stephen J. Anderson,[1] Marianne C. Kramer,[1,2] Sager J. Gosai,[1] Xiang Yu,[1] Lee E. Vandivier,[1,2] Andrew D.L. Nelson,[3] Zachary D. Anderson,[1] Mark A. Beilstein,[3] Rupert G. Fray,[4] Eric Lyons,[3] and Brian D. Gregory[1,2,5,*]
[1]Department of Biology, University of Pennsylvania, Philadelphia, PA 19104, USA
[2]Cell and Molecular Biology Graduate Group, University of Pennsylvania, Philadelphia, PA 19104, USA
[3]School of Plant Sciences, University of Arizona, Tucson, AZ 85721, USA
[4]Plant Sciences Division, School of Biosciences, University of Nottingham, Sutton Bonington Campus, Loughborough LE12 5RD, UK
[5]Lead Contact
*Correspondence: bdgregor@sas.upenn.edu
https://doi.org/10.1016/j.celrep.2018.10.020

SUMMARY

N^6-methyladenosine (m^6A) is a dynamic, reversible, covalently modified ribonucleotide that occurs predominantly toward 3′ ends of eukaryotic mRNAs and is essential for their proper function and regulation. In *Arabidopsis thaliana*, many RNAs contain at least one m^6A site, yet the transcriptome-wide function of m^6A remains mostly unknown. Here, we show that many m^6A-modified mRNAs in *Arabidopsis* have reduced abundance in the absence of this mark. The decrease in abundance is due to transcript destabilization caused by cleavage occurring 4 or 5 nt directly upstream of unmodified m^6A sites. Importantly, we also find that, upon agriculturally relevant salt treatment, m^6A is dynamically deposited on and stabilizes transcripts encoding proteins required for salt and osmotic stress response. Overall, our findings reveal that m^6A generally acts as a stabilizing mark through inhibition of site-specific cleavage in plant transcriptomes, and this mechanism is required for proper regulation of the salt-stress-responsive transcriptome.

Q1 INTRODUCTION

N^6-methyladenosine (m^6A) is the most prevalent internal covalent mRNA modification and has been described in many organisms, including mammals, plants, *Drosophila melanogaster*, and zebrafish (Dominissini et al., 2012; Lence et al., 2016; Luo et al., 2014; Meyer et al., 2012; Zhao et al., 2017). m^6A is indispensable for proper development of many multicellular organisms, as deficiency in enzymes that catalyze and bind m^6A methylation leads to improper development. In zebrafish embryos, m^6A presence results in the destabilization and timely clearance of maternal transcripts from the embryo (Zhao et al., 2017), and in *Drosophila*, m^6A is required for proper sex determination (Lence et al., 2016). In mammalian systems, where m^6A is best characterized, m^6A modulates transcript localization and stability (Wang et al., 2014a).

In *Arabidopsis thaliana* (hereafter *Arabidopsis*), m^6A primarily localizes near the stop codon and throughout the 3′ UTR (Shen et al., 2016), similar to observations in metazoans (Lence et al., 2016; Meyer et al., 2012; Niu et al., 2013). m^6A in *Arabidopsis* occurs nearly exclusively in an RRACH sequence context (Niu et al., 2013; where R = A/G, A is the modified m^6A site, and H = A/C/U). It is estimated that 0.1% of all adenosines present in mRNAs are m^6A (Luo et al., 2014). The primary m^6A methylation writer complex in plants consists of METHYLTRANSFERASE A (MTA) (Zhong et al., 2008), METHYLTRANSFERASE B (MTB) (Zhong et al., 2008), and FKBP INTERACTING PROTEIN 37 (FIP37) (Shen et al., 2016), which all have highly conserved mammalian orthologs; METTL3; METTL14; and Wilm's tumor 1 associated protein, respectively (reviewed in Kramer et al., 2018). m^6A sites are conserved between evolutionarily divergent *Arabidopsis* ecotypes (Luo et al., 2014), suggesting m^6A localization within the transcriptome plays important roles. The importance of m^6A is further emphasized by its necessity in early plant development, as plants deficient for members of the core m^6A methylation complex are embryonic lethal (Shen et al., 2016; Zhong et al., 2008). m^6A has also been implicated in regulating plant response to viral pathogens, where increased levels of m^6A in viral RNAs of the cucumber mosaic virus inhibited systemic invasion (Martínez-Pérez et al., 2017). However, the effects of m^6A on other plant responses, including abiotic stress responses, are not well understood.

Although these studies have clearly demonstrated the importance of m^6A in plants, the mechanisms of m^6A-mediated transcriptome regulation are not currently well understood. For instance, a previous study demonstrated m^6A destabilizes a handful of transcripts in undifferentiated tissue (Shen et al., 2016). However, other studies in a whole organismal context found many transcripts are destabilized when "reader" proteins that bind m^6A are absent (Wei et al., 2018), indicating that m^6A stabilizes mRNAs as well. Thus, whether this epitranscriptome mark stabilizes, destabilizes, or both remains unclear. Furthermore, the mechanisms by which m^6A regulates transcript stability are still not completely clear in any organism.

Here, we use a combination of high-throughput sequencing approaches to reveal that, in plant somatic tissue, m^6A stabilizes transcripts by inhibiting ribonucleolytic cleavage directly 5′ of these modification sites. Furthermore, we show

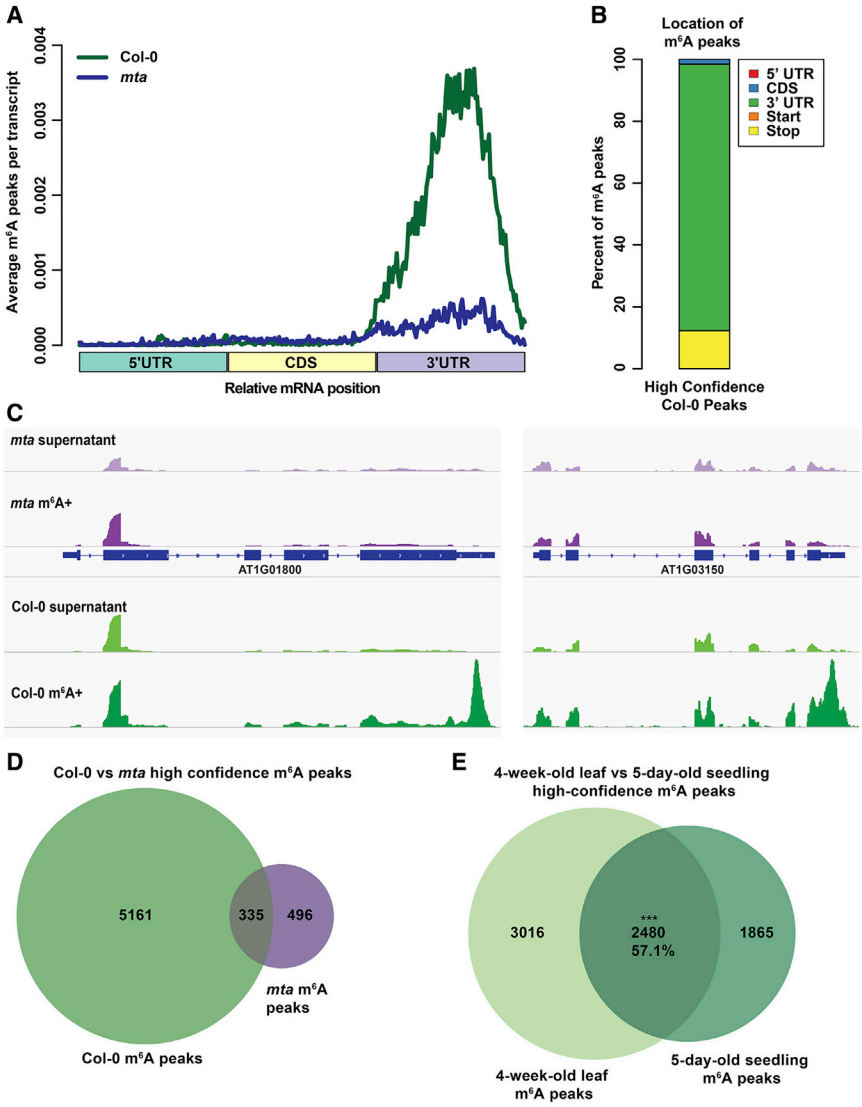

Figure 1. *Arabidopsis* m^{6}A Sites Are Biased toward the 3′ End of mRNAs and Conserved between Distinct Stages of Development

(A) The localization of m^{6}A peaks in Col-0 (green line) and *mta* (purple line) in 4-week-old leaf mRNAs.

(B) Percentage of total Col-0 m^{6}A peaks located throughout regions of mRNA transcripts. Peaks that overlapped a start or stop codon were designated as start or stop codon peaks.

(C) Browser views for two example transcripts containing Col-0 m^{6}A peaks. Top tracks show m^{6}A-seq data for supernatant (top) and m^{6}A+ immunoprecipitation (IP) (bottom) samples using leaf RNA sample from *mta* plants (purple). Bottom two tracks show m^{6}A-seq data for supernatant (top) and m^{6}A+ IP (bottom) samples using leaf RNA sample from Col-0 plants (green).

(D) Overlap between high-confidence m^{6}A peaks identified for Col-0 compared to those from *mta* plants.

(E) Overlap between our 4-week-old Col-0 leaf m^{6}A peaks with peaks from a previous study using 5-day-old whole Col-0 seedlings. *** denotes p value < 0.001 for enrichment in the overlap, chi-square test.

See also Figure S1.

m^{6}A is dynamically added to salt-stress-related transcripts to protect them from degradation upon stressed conditions.

RESULTS

m^{6}A Sites Are Biased toward the 3′ End of mRNAs and Conserved between Distinct Stages of *Arabidopsis* Development

To identify m^{6}A sites in the *Arabidopsis* adult leaf transcriptome, we performed m^{6}A RNA immunoprecipitation and sequencing (m^{6}A-seq) (Meyer et al., 2012) on polyA$^+$ RNA from leaves 5–9 of 4-week-old *Arabidopsis* ecotype Columbia-0 (hereafter Col-0) as well as plants deficient in m^{6}A by virtue of a post-embryonic knockout of the major m^{6}A methyltransferase, MTA (*mta ABI3:MTA*; hereafter referred to as *mta*; Bodi et al., 2012). Using the peak caller MACS2 (Zhang et al., 2008), we identified a total of 9,385 m^{6}A peaks in Col-0 plants, with 5,496 peaks common to both replicates (~87% of peaks in the lower sequencing depth replicate) indicating high reproducibility (Figure S1A; Table S1). Only 2,687 total m^{6}A peaks were identified in *mta* plants, with 831 common to both replicates (Figure S1B), suggesting that mRNA m^{6}A modifications are greatly diminished by decreased MTA abundance. Based on the large number of overlapping m^{6}A peaks identified in Col-0 plants, our analyses focused on only these high-confidence peaks from Col-0 and *mta*.

We found that m^{6}A sites from Col-0 and *mta* plants demonstrated the previously reported bias toward the stop codon and 3′ UTR (Meyer et al., 2012; Shen et al., 2016). In fact, over 95% of the identified Col-0 m^{6}A peaks occur in the 3′ UTR or overlap the stop codon (Figures 1A–1C), and this bias was also observed for the *mta* peaks (Figure 1A), of which only ~40% (335) overlap with Col-0 peaks (Figure 1D). We observed a significant (p value < 0.001; chi-square test) enrichment for the canonical m^{6}A motif (RRACH; Niu et al., 2013) in both Col-0 and *mta* leaf m^{6}A peaks compared to randomly scrambled peak sequences using compareMotifs.pl (Heinz et al., 2010; Figure S1C). These findings indicate that we identified high-confidence m^{6}A-containing regions of the *Arabidopsis* mature leaf transcriptome. Additionally, our results revealed that *mta* plants provide an m^{6}A-deficient background to probe the effects of this mark on the plant transcriptome.

To characterize what processes may be regulated by m^{6}A in adult leaves, we performed a Gene Ontology (GO) analysis using DAVID on transcripts containing Col-0 m^{6}A peaks. We found that these transcripts are enriched for genes encoding proteins

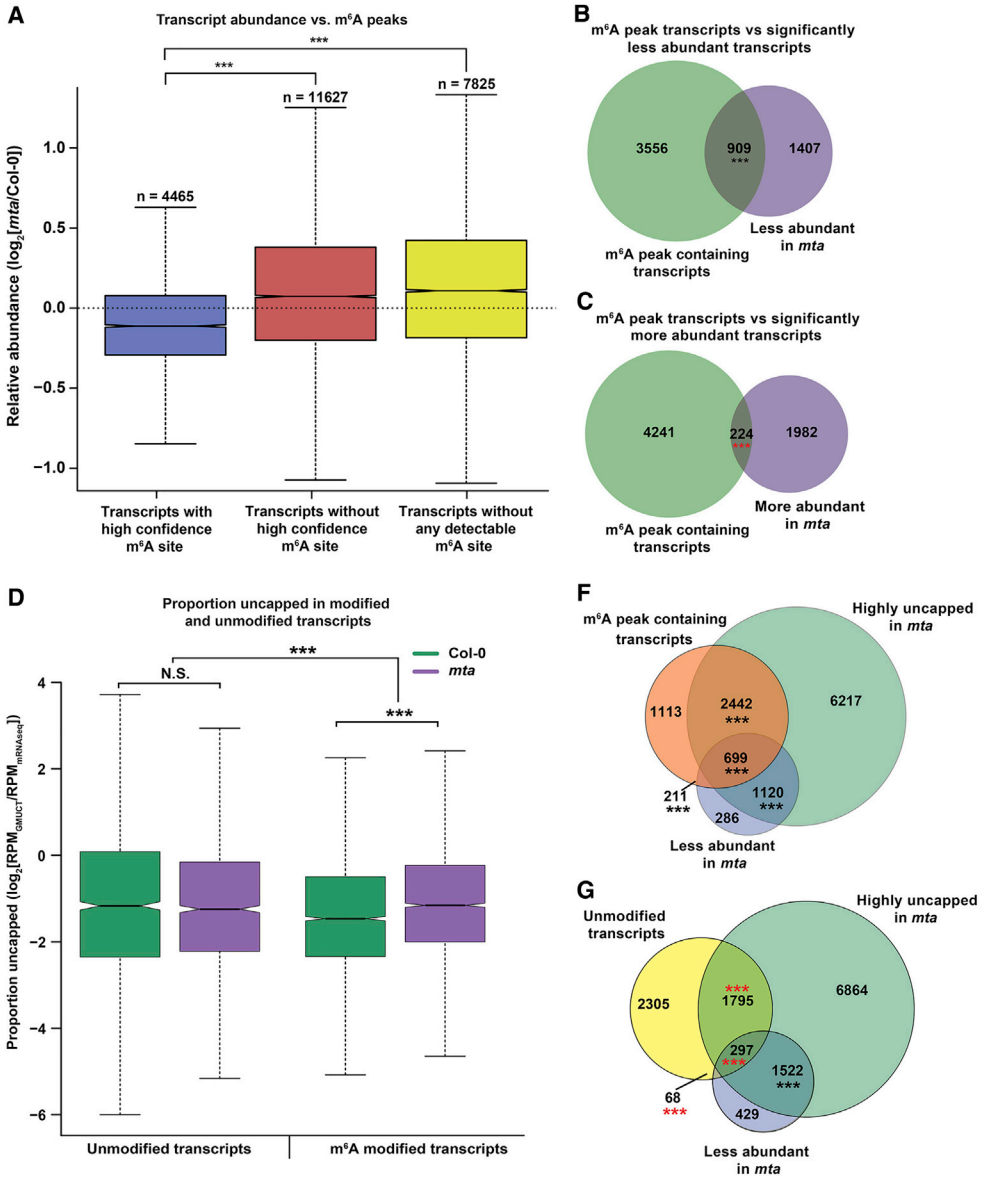

(legend on next page)

Please cite this article in press as: Anderson et al., N^6-Methyladenosine Inhibits Local Ribonucleolytic Cleavage to Stabilize mRNAs in *Arabidopsis*, Cell Reports (2018), https://doi.org/10.1016/j.celrep.2018.10.020

involved in metabolism and growth (Table S2). These results support the importance of m^6A as a regulator of the plant development and metabolism.

m^6A is critical for proper eukaryotic development (Lence et al., 2016; Wang et al., 2014b; Zhao et al., 2017; Zhong et al., 2008), but whether m^6A sites are maintained across plant development is not known. Therefore, we compared our Col-0 4-week-old leaf m^6A sites to those from an m^6A-seq experiment that used 5-day-old Col-0 whole seedlings (Shen et al., 2016). We found a significant (p value < 0.001; chi-square test) overlap of m^6A peaks between both developmental stages (2,480; ~57% of the total 5-day-old seedling set; Figure 1E), indicating that m^6A is essential for both regulating development (Shen et al., 2016) and general transcriptome maintenance during plant development. This is further supported by the GO analysis that revealed many transcripts containing m^6A encode proteins involved in general processes (Table S2).

m^6A-Modified Protein-Coding mRNAs Are Significantly Less Abundant and Stable in the Absence of this Epitranscriptome Mark

Multiple studies in mammalian stem cells suggested that m^6A acts largely as a destabilizing mark (Wang et al., 2014a, 2014b). In plants, the effects of m^6A are less clear (Duan et al., 2017; Shen et al., 2016). In order to more comprehensively investigate the effects of m^6A on the abundance of modified transcripts in adult leaf tissue, we performed $polyA^+$-selected RNA sequencing (mRNA-seq) using RNA from leaves 5–9 of 4-week-old Col-0 and *mta* plants. The resulting mRNA-seq libraries were sequenced and provided ~27–40 million mapped reads per library. A principal-component analysis (PCA) (Anders et al., 2015) of read coverage using HTseq accompanied with DESeq2 (Love et al., 2014) revealed the high quality and reproducibility of our mRNA-seq libraries (Figure S2A).

We then calculated the relative abundance (reads per million [RPM]) in the absence compared to the presence of m^6A ($RPM_{mta}/RPM_{Col\text{-}0}$) for transcripts with one or more high-confidence m^6A peaks, transcripts without any high confidence Col-0 m^6A peaks, and transcripts without any Col-0 m^6A peaks in either m^6A-seq replicate. We observed a significant (p value < 0.001; chi-square test) decrease in overall transcript abundance when m^6A is absent (*mta*) compared to present (Col-0) in transcripts containing m^6A peaks as compared to the other two classes of transcripts (Figure 2A). In fact, m^6A peak-containing transcripts decrease in abundance in the absence of this mark (median < 0), whereas the other two classes of transcripts slightly increase in abundance (median > 0; Figure 2A).

We next identified transcripts that demonstrated significant changes in abundance between *mta* and Col-0 plants using the differential expression analysis suite DEseq2 (Love et al., 2014). ~4,522 mRNAs were identified as differentially abundant in *mta* plants as compared to Col-0. Nearly half of the significantly (false discovery rate [FDR] $\leq$ 0.05) differentially abundant genes showed higher levels (2,206) in *mta* compared to Col-0, and the other half (2,316) were decreased (Table S3). We validated the DESeq2 results using qRT-PCR on 12 randomly selected significantly differentially abundant transcripts. These qRT-PCR results were highly correlated (R = 0.94; Pearson's correlation coefficient) with the fold change in abundance determined by DESeq2 (Figure S2B), validating our differential expression analysis. We next assessed the level of association between mRNAs with significant changes in abundance and those that contain m^6A peaks. Of the 2,316 transcripts less abundant in *mta* plants, 910 (39%) contained at least one m^6A site in Col-0, which is significantly (p value < 0.001; hypergeometric test) more than expected (Figures 2B and S2C). Conversely, only 224 (10%) of the transcripts more abundant in *mta* compared to Col-0 plants (2,206 total) contained at least one m^6A peak, which is significantly (p value < 0.001; hypergeometric test) less than expected (Figures 2C and S2C). No association was observed for differential abundance and transcripts containing *mta* m^6A peaks (Figures S2D and S2E). These data reveal that m^6A is predominately found in mRNAs that are down-regulated upon its loss, suggesting that it is primarily a stabilizing mark in plant transcriptomes.

Figure 2. m^6A-Modified Protein-Coding mRNAs Are Significantly Less Abundant and Stable in m^6A-Deficient Plants

(A) Relative abundance of transcripts containing high-confidence Col-0 m^6A peaks (blue box; N = 4,510), no high-confidence Col-0 m^6A peaks (red box; N = 11,627), and no detectable m^6A peaks in any replicate (yellow box; N = 7,825). Transcript abundance is shown as the log_2 fold change in *mta* reads per million (RPM) divided by Col-0 RPM. *** denotes p value < 0.001; chi-square test.

(B) Overlap between Col-0 m^6A peak containing protein-coding mRNAs with those that are significantly less abundant in *mta* as compared to Col-0 leaves. *** denotes p value < 0.001 for enrichment in the overlap; chi-square test.

(C) Overlap between Col-0 m^6A peak containing protein-coding mRNAs with those that are significantly more abundant in *mta* as compared to Col-0 leaves. *** denotes p value < 0.001 for less than expected in the overlap; chi-square test.

(D) Proportion uncapped (GMUCT RPM normalized to RNA-seq RPM for each mRNA) for transcripts that contain (left) no detectable Col-0 m^6A peaks and (right) Col-0 m^6A peaks in Col-0 (green boxes) compared to *mta* (purple boxes) leaves. *** denotes p value < 0.001; Wilcoxon ranked sum test.

(E) Percent of transcripts remaining 24 hr post-treatment with transcription inhibitors in Col-0 (green bars) and *mta* (purple bars). The indicated classes of m^6A-modified transcripts were chosen from our proportion uncapped data and assayed. * denotes p value < 0.05, ** denotes p value < 0.01, and N.S. denotes not significant; Student's t test, two-tailed. Error bars represent SE.

(F) Overlap between transcripts containing Col-0 m^6A peaks (red circle), transcripts that have an increase in proportion uncapped in *mta* compared to Col-0 (green circle), and transcripts that are significantly less abundant in Col-0 (blue circle). *** denotes a significant (p value < 0.001) overlap between the specified transcript populations; log-linear analysis.

(G) Overlap between randomly chosen transcripts (a number equal to m^6A containing transcripts) that do not contain detectable Col-0 m^6A peaks (yellow circle), transcripts that have an increase in proportion uncapped in *mta* compared to Col-0 (green circle), and transcripts that are significantly less abundant in Col-0 (blue circle). *** denotes a significant (p value < 0.001) overlap between the specified transcript populations; log-linear analysis. *** denotes p value < 0.001 for less than expected in the overlap; log-linear analysis.

See also Figure S2.

To assess what biological processes may be affected in the absence of m^6A, we performed a GO analysis using DAVID (Huang et al., 2009) on transcripts that were significantly differentially abundant in *mta* compared to Col-0. Interestingly, defense response and a variety of stress terms were pervasive in both over- and underrepresented transcripts. These GO terms spanned diverse biotic and abiotic stresses, including response to bacterial, fungal, insect, heat, and salt stress (Table S2). These GO terms suggest that m^6A regulates a wide range of stress response pathways by ensuring the appropriate abundance of necessary mRNAs.

To further investigate whether m^6A is a stabilizing mark in plants, we performed global mapping of uncapped and cleaved transcripts (GMUCT) (Gregory et al., 2008; Willmann et al., 2014) to quantify the degradation and cleaved intermediates of $polyA^+$ transcripts in leaves 5–9 of 4-week-old Col-0 and *mta* plants. The resulting GMUCT libraries were sequenced and provided ~79–82 million mapped reads per library. We then performed a PCA using HTseq and DESeq2 (Love et al., 2014), which revealed high reproducibility of our GMUCT libraries (Figure S2F).

These GMUCT results were used to characterize the relative stability of transcripts using the proportion uncapped metric, which is the $\log_2$ ratio of the RPM from GMUCT for a given transcript normalized by the RPM for that same transcript in our mRNA-seq data ($\log_2[RPM_{GMUCT}/RPM_{mRNaseq}]$). This proportion uncapped metric was previously shown to be a good measure of mRNA stability (Vandivier et al., 2015), where a higher proportion uncapped value correlates with a less stable transcript and vice versa. Using this metric, we compared the influence of m^6A on transcript stability by comparing proportion uncapped in Col-0 and *mta* plants for transcripts that contain m^6A (m^6A modified) or do not (unmodified). To avoid confounding proportion uncapped values found at the extreme ends of abundance, we excluded the top and bottom 12.5% most expressed m^6A containing transcripts (Figure S2C). We found a significant (p value < 0.001; Wilcoxon rank sum test) increase in proportion uncapped for m^6A-modified transcripts in *mta* compared to Col-0 plants, indicating that these transcripts are less stable when m^6A is absent (Figure 2D). Conversely, we observed no significant change in proportion uncapped between Col-0 and *mta* for similarly expressed and non-significantly differentially abundant transcripts lacking detectable m^6A modification (Figure 2D).

To validate our proportion uncapped stability results, we treated Col-0 and *mta* plants with the transcription inhibitors cordycepin and actinomycin D for 0 and 24 hr. Because these inhibitors cannot penetrate the thick epidermal layer of 4-week-old leaves, we performed this analysis in 5-day-old seedlings as many m^6A sites are shared between these two tissues (Figure 1E). Using transcripts with m^6A peaks shared between these two tissues, we tested the stability of several mRNAs, which exhibited higher levels of proportion uncapped in *mta* compared to Col-0. We then calculated the percentage of initial transcripts remaining 24 hr after treatment using qRT-PCR and found that these mRNAs were significantly more stable in Col-0 compared to *mta* (Figure 2E). Our stability assay was also able to validate two mRNAs exhibiting <10% fold change in proportion uncapped between *mta* and Col-0 and one transcript that demonstrated a substantial increase in proportion uncapped in *mta* relative to Col-0 (Figure 2E). These results indicate m^6A is generally a stabilizing mark in plant transcriptomes.

We hypothesized that m^6A-associated transcript stability was driving the abundance changes between Col-0 and *mta* plants. To test this, we determined the overlap between transcripts with an m^6A site, differentially abundant transcripts, and transcripts that were either stabilized or destabilized in *mta* as compared to Col-0 plants. We found a striking and significant (p value < 0.001; log-linear analysis) association between transcripts significantly less abundant in m^6A-deficient plants, transcripts destabilized in m^6A-deficient plants, and transcripts m^6A modified in Col-0, but not *mta*, plants (Figure 2F; Table S3). Conversely, a randomly selected equally sized subset of transcripts unmodified in Col-0 were significantly (p value < 0.001; log-linear analysis) under-enriched in the population of mRNAs that are less abundant and stable in m^6A-deficient plants (Figure 2G). Relatedly, the populations of m^6A-modified mRNAs are significantly (p value < 0.001; log-linear analysis) disassociated from mRNAs that are more abundant and/or more stable in *mta* as compared to Col-0 plants, whereas unmodified transcripts show no such dissociation (Figures S2G–S2J). Overall, our results indicate that the decrease in abundance of mRNAs that lose methylation in m^6A-deficient plants is often due to the loss of m^6A's stabilizing effect.

m^6A Modification on mRNAs Inhibits Local Ribonucleolytic Cleavage

Because m^6A is added directly onto the primary sequence of mRNAs, we investigated whether m^6A has a local effect on ribonucleolytic cleavage of modified transcripts using our GMUCT data. To do this, we quantified only the reads mapping within m^6A peaks in GMUCT compared to mRNA-seq for *mta* compared to Col-0 plants and looked for significant increases and decreases in local cleavage levels. 1,539 m^6A peaks demonstrated a significant (FDR < 0.05; chi-square test) increase in cleavage (increase in GMUCT compared to mRNA-seq) in m^6A-deficient relative to Col-0 plants (Figure 3A). Conversely, only 198 peaks demonstrated a significant (FDR < 0.05; chi-square test) increase in cleavage level in Col-0 relative to *mta* plants (Figure 3A).

To test the generality of this phenomenon, we assessed cleavage levels within all m^6A peaks in Col-0 compared to *mta* plants. In GMUCT, the 5′ adaptor is directly added to the nucleotide immediately downstream of cleavage; thus, the 5′ end of each sequencing read represents the cleavage site (Willmann et al., 2014). Therefore, we defined a cleavage score as the RPM coverage values for the 5′ most nucleotide of all GMUCT reads. We observed a significant (p value < 0.001; Wilcoxon ranked sum test) increase in ribonucleolytic cleavage within 50 nt of m^6A peak centers in *mta* compared to Col-0 plants (Figure 3B), indicating that sites with m^6A in Col-0, but not in *mta*, are more cleaved when the modification is absent. These results revealed that m^6A generally prevents local ribonucleolytic cleavage of *Arabidopsis* adult leaf mRNAs. To determine whether this cleavage was specific to m^6A sites and not higher throughout transcripts that lose m^6A in *mta* plants, we calculated the $\log_2$

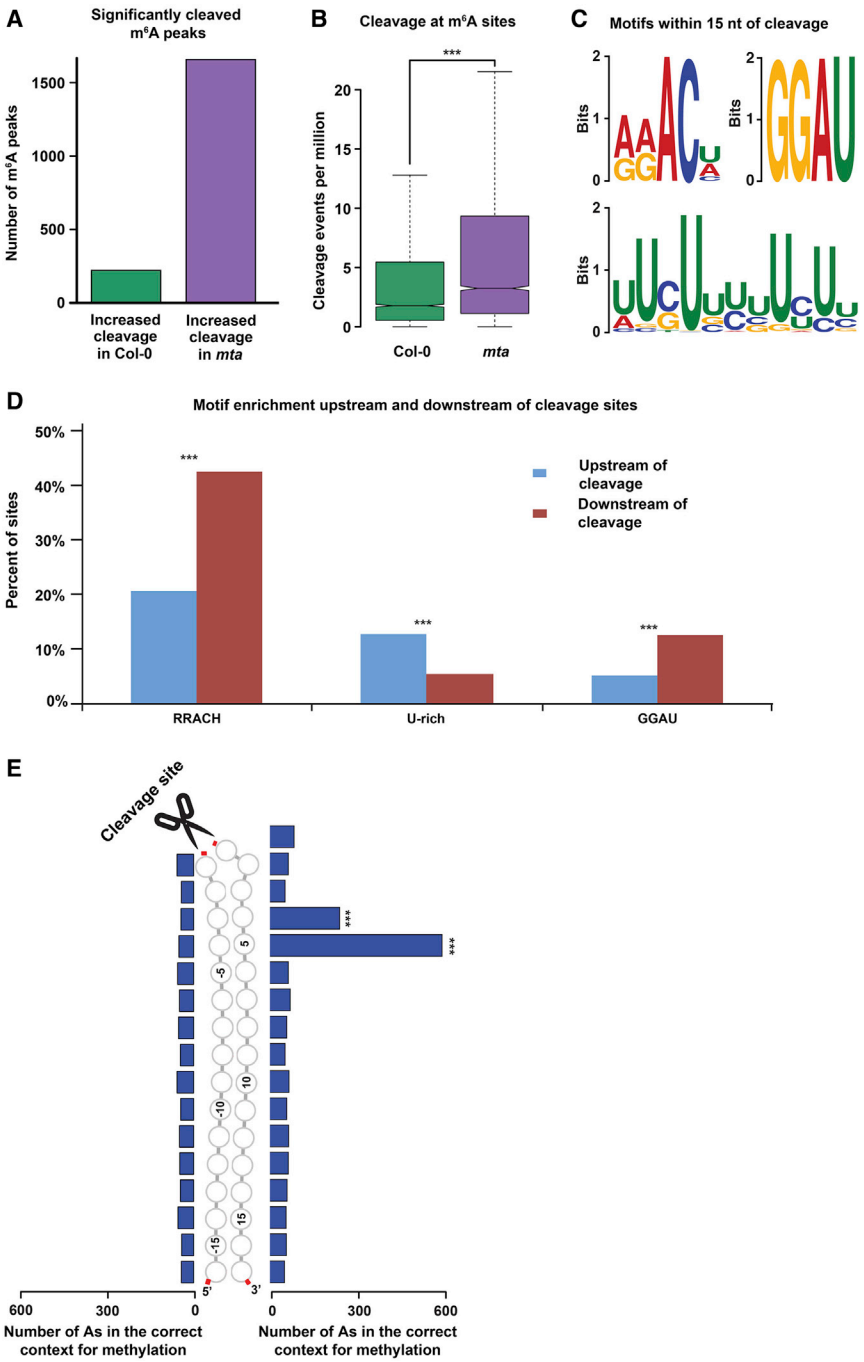

Figure 3. m^{6}A Modification on Protein-Coding mRNAs Inhibits Local Ribonucleolytic Cleavage 4 or 5 nt Upstream of m^{6}A Sites

(A) Number of Col-0 m^{6}A peaks that are significantly less cleaved in *mta* relative to Col-0 (green bar) compared to the opposite cleavage pattern (purple bar).

(B) Number of normalized cleavage events occurring in Col-0 m^{6}A peaks as determined using GMUCT 5′ read ends from Col-0 (green box) as compared to *mta* (purple box) adult leaf libraries. *** denotes p value < 0.001; Wilcoxon ranked sum test.

(C) Three motifs discovered within 15 nt of the highest cleaved nucleotide within m^{6}A peaks. The motif on the top left represents the canonical m^{6}A motif, the motif on the bottom left is a U-rich motif that represent sites of protein binding, and the motif on the top right appears to be a non-canonical m^{6}A motif.

(D) Enrichment of the specified motifs (x axis) within 25 nt up- (blue bars) and downstream (red bars) of the most cleaved nucleotide in Col-0 m^{6}A peaks. *** denotes p value < 0.001; chi-square test.

(E) The number of As that occur in the RRACH context in the immediate vicinity of the most cleaved nucleotide within Col-0 m^{6}A peaks. The scissors denote the most cleaved nucleotide. Circles to the left of the scissors represent nucleotides 5′ of the cleavage site, and those to the right are nucleotides 3′ of these sites. Only the first A found in this sequence context in both directions is counted on this graph. *** denotes nucleotides with p values < 0.001; chi-square test.

See also Figure S3.

ratio of cleavage between m^{6}A-deficient and Col-0 plants in m^{6}A peaks compared to same-sized windows 300 nt upstream of these peaks and to randomly selected sites toward the 3′ end of unmodified transcripts. We found a significant (p value < 0.001; Wilcoxon ranked sum test) increase in the $\log_2$ *mta*/Col-0 cleavage score ratio for m^{6}A peaks as compared to both sets of control regions (Figure S3A). These findings indicate that the loss of m^{6}A in *mta* mutant plants results in increased local cleavage.

XRN4 Is Responsible for Degrading the Downstream Products of m^{6}A-Regulated Cleavage

We observed an accumulation of mono-phosphorylated 5′ ends occurring specifically within m^{6}A peaks (Figure 3B). Therefore, we asked whether EXORIBONUCLEASE4 (XRN4), a 5′-to-3′ exoribonuclease that degrades 3′ fragments occurring after microRNA-mediated cleavage of target mRNAs (Souret et al., 2004), is also involved in degrading 3′ cleavage products at m^{6}A sites. To do this, we took the cleavage scores within 25 nt of the most cleaved nucleotides in *mta* plants found in Col-0 m^{6}A peaks and compared them to an arbitrary region 300 nt closer to the 5′ end of the transcript for *xrn4* and Col-0 plants. If XRN4 degrades downstream cleavage products, we expected more GMUCT reads around m^{6}A-regulated cleavage sites in *xrn4* compared to Col-0 (Figure S3B). We observed a significant (p value < 0.001; Wilcoxon ranked sum test) accumulation of 5′ GMUCT read ends near m^{6}A cleavage sites as compared to the upstream sites in *xrn4* mutant plants, whereas no significant difference was observed in Col-0 (Figure S3C). To control for the

possibility that 3′ ends of transcripts are generally overrepresented in *xrn4* GMUCT libraries, we performed the same analysis on random 50-nt windows in the 3′ UTR of transcripts that contained no detectable m^{6}A. We observed little difference between accumulation of read ends at or upstream of these random sites in both *xrn4* and Col-0 plants (Figure S3C). In total, these results reveal that XRN4 degrades the 3′ cleavage fragments generated by m^{6}A-regulated cleavage (Figure S3B).

Cleavage in the Absence of m^{6}A Occurs 4 or 5 nt Upstream of Unmodified As

We looked for enriched sequences that might explain this m^{6}A-regulated cleavage. To do this, we calculated the nucleotide with the most coverage of *mta* 5′ GMUCT read ends within each m^{6}A peak found in Col-0, but not *mta*, plants, revealing the m^{6}A-regulated cleavage site. Nearly all Col-0 m^{6}A peaks (5,456/5,496; 99%) had at least one highly cleaved nucleotide in m^{6}A-deficient (*mta*) plants. We then took the 7 nt up and downstream (15 nt total) of these sites and ran the motif discovery algorithm MEME (Bailey et al., 2009) to characterize sequences associated with m^{6}A-regulated cleavage. Strikingly, this motif search returned the canonical m^{6}A motif RRACH and a GGAU motif (Figure 3C), indicating these cleavage events occur locally near *Arabidopsis* adult leaf m^{6}A sites. We also found a U-rich motif in this 15-nt window around cleavage sites (Figure 3C). Of note, none of these motifs were found when MEME was run using 15-nt regions around m^{6}A peak centers or randomly selected peak regions, so these findings are likely not the result of general RRACH enrichment in our m^{6}A peaks (Figure S1C). We also found that these sites were cleaved in Col-0 plants but to a much lower extent (Figure 3B).

To assess positional preference for these enriched motifs with respect to m^{6}A-regulated cleavage sites, we investigated sequences 25 nt 5′ and 3′ of each of these highly cleaved positions. We used "homer2 known" (Heinz et al., 2010) to compare the relative enrichment of GGAU, U-rich (UUUUU), and RRACH motifs in these regions. We observed a significant enrichment (p value < 0.001; chi-square test) for the RRACH and GGAU sequence motifs 3′ of m^{6}A-regulated cleavage sites, whereas the U-rich motif was significantly (p value < 0.001; chi-square test) enriched 5′ of these sites (Figure 3D), indicating significant sequence preferences around m^{6}A-regulated cleavage sites.

To elucidate whether there was an optimal distance from an RRACH sequence for these cleavage sites, we calculated the number of "modifiable" adenosines (the A in an RRACH context) occurring at each position up- and downstream of m^{6}A-regulated cleavage sites. We found a clear bias for cleavage at positions four and five nucleotides 5′ of a modifiable A (Figure 3E), and this bias was significant (p value < 0.001; chi-square test) relative to all other nucleotides flanking these highly cleaved sites. Furthermore, a cross-linking induced mutation sites (CIMS)-based analysis (Linder et al., 2015) of these regions suggests these modifiable As are methylated in Col-0 and not in *mta* plants (Figure S3D). We also found a bias for As occurring within the GGAU motif (Figures S3E and S3F), suggesting GGAU may be a non-canonical *Arabidopsis* m^{6}A motif. The polyA$^+$ selection step of the GMUCT protocol may bias our findings of ribonucleolytic cleavage near m^{6}A sites that are mostly 3′ UTR localized. However, this is unlikely due to the nucleotide specificity of our findings and strong GMUCT coverage substantially 5′ of these regions. In total, our findings reveal that m^{6}A generally stabilizes *Arabidopsis* leaf mRNAs by directly inhibiting local ribonucleolytic cleavage, providing insight into a pervasive mechanism regulating mRNA stability in *Arabidopsis*. This mechanism was evident when we inspected browser views of GMUCT, mRNA-seq, and m^{6}A-seq reads at m^{6}A cleavage sites in *mta* compared to Col-0 plants (Figures 5A and S5A).

Dynamic m^{6}A Addition Stabilizes Transcripts Encoding Salt Response Proteins during Response to this Abiotic Stress

We found that differentially abundant transcripts in *mta* compared to Col-0 are enriched for those encoding proteins involved in salt stress response (Table S2). Therefore, we tested whether m^{6}A regulated these mRNAs during agriculturally relevant salt stress treatments. To do this, we grew wild-type *Arabidopsis* plants for 2 weeks on soil under normal watering conditions. Subsequently, we continued watering them with normal water (control conditions) or by watering *Arabidopsis* plants with 50 mM NaCl followed by 100 mM NaCl three days later (salt conditions). For salt conditions, we then watered with 150 mM NaCl every three days for a total of four treatments (Figure S4A). At the conclusion of treatments, we collected the ~4-week-old rosette leaves for all subsequent experiments.

To determine the effects of these treatments on m^{6}A deposition, we performed m^{6}A-seq using polyA$^+$ RNA from both control- and salt-treated 4-week-old leaves. Using the peak caller MACS2 (Zhang et al., 2008), we identified a total of 23,009 and 25,448 m^{6}A peaks in control- and salt-treated samples, respectively. Of these, 15,106 (79.4%) and 17,848 (84.8%) peaks were identified in both biological replicates of control and salt, respectively (high-confidence peaks; Figure 4A; Table S4). Although 88.5% of these high-confidence m^{6}A peaks overlap for both treatment conditions, we also identified 1,731 and 4,473 m^{6}A peaks that are unique to control (control-specific) and salt treatments (salt-specific), respectively (Figure 4A; Table S4). As expected, m^{6}A peaks identified for both conditions were enriched in the 3′ UTR and stop codon regions (Figures S4B and S4C).

To characterize the transcripts with control- or salt-specific m^{6}A peaks, we performed a GO analysis using DAVID (Huang et al., 2009) on mRNAs with m^{6}A peaks only in control or salt conditions (989 and 3,691, respectively). We found that genes encoding proteins involved in water deprivation, response to osmotic and salt stress, and response to karrikin display salt-specific m^{6}A peaks (Figure 4B; Table S2). Conversely, genes with control-specific m^{6}A peaks were enriched for more general terms, such as photosynthesis, photorespiration, and response to cytokinin (Figure 4B; Table S2). These results reveal that, upon salt stress, transcripts encoding salt and osmotic stress response proteins gain m^{6}A.

Because m^{6}A stabilizes transcripts by decreasing ribonucleolytic cleavage, we hypothesized that m^{6}A protects salt-responsive transcripts via this mechanism upon salt stress. To test this, we performed GMUCT and mRNA-seq using RNA samples from control- and salt-treated 4-week-old leaves. The resulting

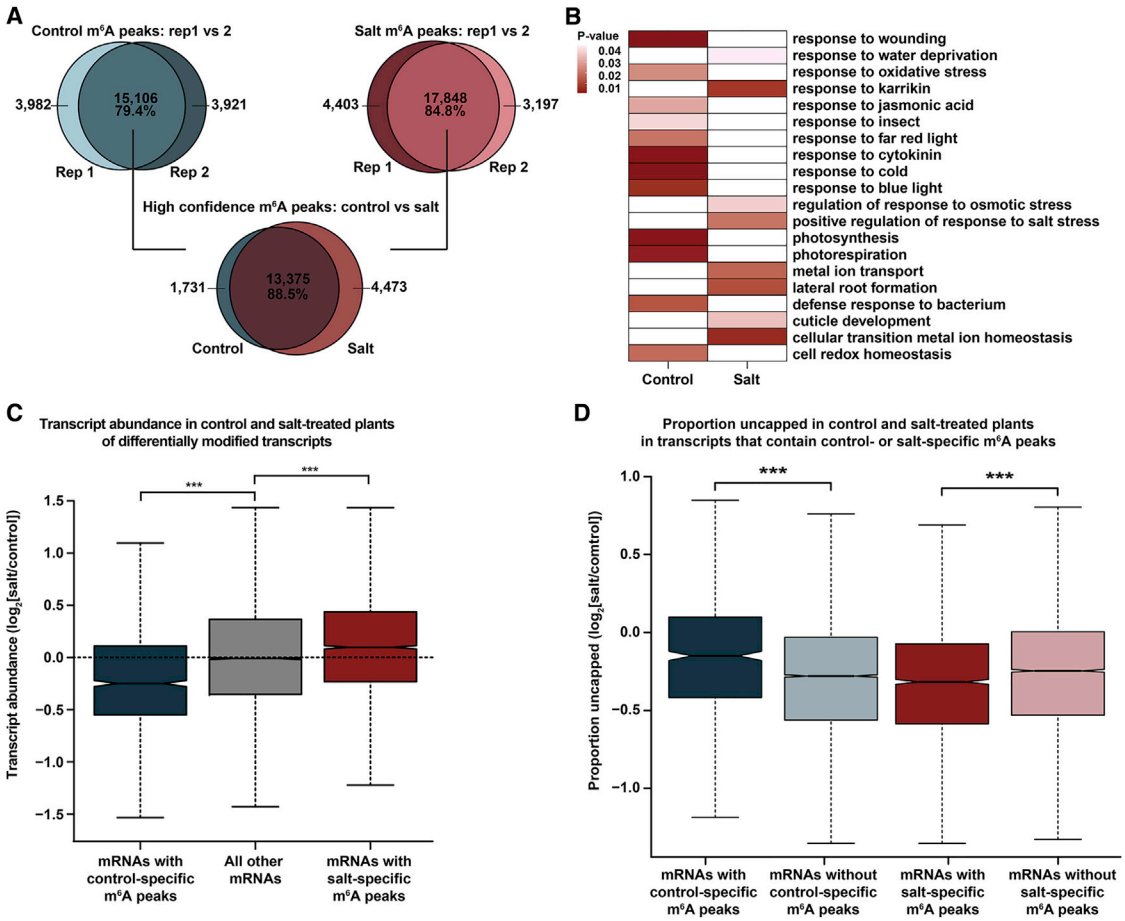

Figure 4. Salt Stress Induces Changes in Transcriptome-wide m^{6}A Deposition, Resulting in Stabilization of the Newly Methylated Transcripts

(A) (Top) Overlap of m^{6}A peaks called by MACS2 between biological replicates of control- (blue circles) and salt (red circles)-treated *Arabidopsis* plants. Intersection of replicates indicates high-confidence m^{6}A peaks. (Bottom) Overlap between control (blue) and salt (red) treatment high-confidence m^{6}A peaks is shown.

(B) Heatmap of Gene Ontology (GO) enrichment terms for transcripts that contain control- (left) or salt-specific (right) m^{6}A peaks. Heatmap colors correspond to p values associated with each GO term.

(C) Relative abundance of transcripts in salt- compared to control-treated plants (salt divided by control) that contain control- (blue box) or salt-specific (red box) m^{6}A peaks or all others (gray box).

(D) Relative levels of proportion uncapped for transcripts in salt compared to control-treated plants (salt divided by control) for transcripts that contain a control-specific m^{6}A site (dark blue box) compared to those that do not (light blue box) as well as in transcripts that contain a salt-specific m^{6}A site (dark red box) compared to transcripts that do not (light red box).

*** denotes p value < 0.001; Wilcoxon ranked sum test. See also Figures S4 and S5.

GMUCT and mRNA-seq libraries provided ~68–95 million single-end reads and ~28–31 million paired-end mapped reads per library, respectively. To determine reproducibility, we used a PCA using HTseq accompanied with DESeq2 (Love et al., 2014) that indicated the high quality and reproducibility of our GMUCT and mRNA-seq libraries (Figures S4D and S4E).

We then compared transcript abundance during salt and control conditions (salt mRNA-seq RPM divided by control mRNA-seq RPM) for mRNAs that have control- or salt-specific m^{6}A peaks as compared to all other genes as a control. We found that transcripts containing salt-specific m^{6}A peaks are significantly (p value < 0.001; Wilcoxon t test) more abundant than those with control-specific m^{6}A peaks as well as all other mRNAs detected by our mRNA-seq experiments ($\log_2$[salt mRNA-seq RPM divided by control mRNA-seq RPM] > 1; Figure 4C; Table S3). Conversely, transcripts with control-specific m^{6}A peaks are less abundant than the general population of mRNAs in salt compared to control conditions (Figure 4C; Table S3). In total, these results demonstrate that m^{6}A deposition on transcripts encoding salt response proteins increases their abundance specifically during salt stress response.

To determine whether this increase in abundance of transcripts containing salt-specific m^{6}A peaks was due to increased stability, we again calculated the proportion uncapped metric for each transcript in both control and salt treatment. We then took the $\log_2$ ratio of proportion uncapped in salt compared to

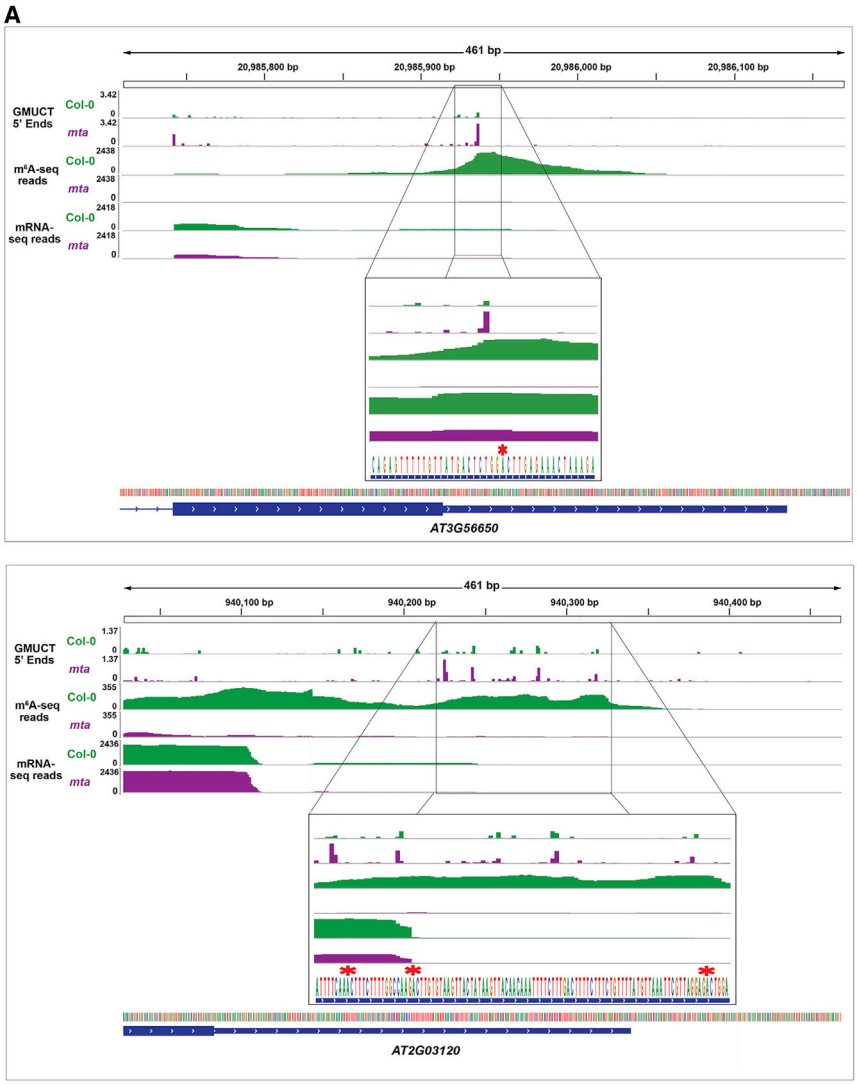

Figure 5. Browser Views and Model of m^{6}A-Regulated Ribonucleolytic mRNA Cleavage and Subsequent Turnover

(A) Browser views of two example transcripts demonstrating increased proportion uncapped and cleavage 4 and 5 nt upstream of RRACH motifs (red asterisks) and reduced expression. Both of these examples were validated as being less stable in our stability time course assay (Figure 3B).

(B) Our results suggest a model in which the absence of m^{6}A induces endonucleolytic cleavage 4 and 5 nt upstream of the now unmodified adenosine by a currently unidentified endoribonuclease. This cleavage results in transcript intermediates that can be degraded by the normal 5′–3′ and 3′–5′ degradation machineries (XRN4 and the exosome, respectively).

(C) Upon salt stress, m^{6}A is dynamically added to transcripts encoding salt stress response proteins, preventing their degradation (bottom). Conversely, the lack of methylation on these transcripts during control treatment allows cleavage-mediated destabilization (top). The m^{6}A-mediated transcript stabilization likely results in increased translation so the proteins can confer proper salt stress response.

See also Figures S1, S2, S3, S4, and S5.

control conditions to examine the stability of transcripts with control- or salt-specific m^{6}A peaks. We found that transcripts with control-specific m^{6}A peaks are significantly (p value < 0.001; Wilcoxon t test) more degraded and cleaved (higher proportion uncapped) than transcripts without these sites in salt as compared to control treatments (Figure 4D). Conversely, transcripts with salt-specific m^{6}A peaks display significantly (p value < 0.001; Wilcoxon t test) lower proportion uncapped and thus are more stable than transcripts without these sites (Figure 4D). In total, our findings reveal that m^{6}A is dynamically and specifically deposited on transcripts encoding salt and osmotic stress response proteins upon agriculturally relevant salt treatment, where its presence promotes abundance and stability of these mRNAs.

DISCUSSION

Despite the prevalence of m^{6}A throughout the transcriptomes of many model organisms, few high-throughput studies have elucidated the mechanisms by which m^{6}A regulates mRNA, and low-throughput mechanistic studies thus far rarely show the scope of that mechanism. Our study establishes a molecular mechanism by which m^{6}A regulates plant mRNA stability in the 4-week-old leaf transcriptome. Specifically, our study revealed that m^{6}A generally acts as a stabilizing factor in *Arabidopsis* leaf mRNAs through the widespread prevention of local ribonucleolytic cleavage, especially during salt

Please cite this article in press as: Anderson et al., N^6-Methyladenosine Inhibits Local Ribonucleolytic Cleavage to Stabilize mRNAs in *Arabidopsis*, Cell Reports (2018), https://doi.org/10.1016/j.celrep.2018.10.020

stress response, where m^6A is specifically deposited on salt-responsive transcripts, increasing their stability.

Our m^6A-seq experiments demonstrated, as was previously suggested (Bodi et al., 2012), that MTA has a major role in adding m^6A to *Arabidopsis* mRNAs (Figures 1A–1D). We also showed consistent maintenance of m^6A modifications between 5-day-old whole seedlings (Shen et al., 2016) and 4-week-old leaves (Figure 1E). This finding, along with the GO analysis of transcripts that contain m^6A in the leaf transcriptome (Table S2), suggests that m^6A regulates development and differentiation as well as basic metabolism during the plant life cycle.

Previous *Arabidopsis* m^6A studies demonstrated an association between m^6A loss and an increase in mRNA abundance through stabilization of specific transcripts, but this does not appear to be the transcriptome-wide trend (Duan et al., 2017; Shen et al., 2016). Furthermore, more recent studies in somatic transcripts demonstrate an association between m^6A and the stabilization of most modified transcripts (Wei et al., 2018). This destabilization occurs in the absence of ECT2, a member of the YTH protein family that directly binds m^6A modifications. Here, we clearly demonstrate that, when 4-week-old leaf transcripts containing m^6A peaks lose this mark, the result is commonly a decrease in transcript abundance via destabilization (Figure 2). Thus, this destabilization may be accomplished by a decrease in m^6A binding by YTH proteins (e.g., ECT2) or other RBPs that normally provide occlusion of the nearby cleavage site. Interestingly, the enrichment of U-rich sequences around m^6A-regulated cleavage sites suggests a potential regulatory role for heterogeneous nuclear ribonucleoproteins (HNRNPs), because they are known to bind U-rich tracts on mRNA near m^6A modifications (Liu et al., 2015). Future work will be directed at addressing these questions.

We also found a number of transcripts whose abundance and stability increases in the absence (*mta*) as compared to presence of m^6A (Col-0) in mature leaves, many of which were also less cleaved in *mta* (Figures 2D, 2E, S2I, and S2J). Thus, the previous studies as well as ours suggest that m^6A is a mostly stabilizing mark on plant mRNAs but also destabilizes a handful of specific target RNAs to affect different biological processes. Uncovering the mechanisms differentiating these two fates of modified transcripts requires further testing.

Although previous studies have demonstrated the widespread effects of m^6A on the transcriptome, most lack a clear mechanism for any regulatory outcomes (Batista et al., 2014; Bodi et al., 2012; Shen et al., 2016; Wang et al., 2014a). Here, we clearly demonstrate that m^6A generally stabilizes transcripts (Figures 1 and 2). This stabilization is due to an inhibition of ribonucleolytic cleavage 4 and 5 nt directly upstream of m^6A sites that we found occurs in RRACH and GGAU sequence contexts (Figures 3, 4, 5, and S3). Although we cannot be entirely sure that this is endonucleolytic as compared to the processive 5′–3′ exonucleolytic cleavage by an enzyme, such as XRN4, that has been blocked by factors associating around m^6A sites, the specificity of the signal occurring precisely 4 and 5 nt upstream of m^6A sites suggests this is highly specific endonucleolytic cleavage performed by some unknown endoribonuclease (Figures 5C and S5B). In total, our results provide a clear mechanism of local cleavage inhibition by m^6A, resulting in mRNA stabilization in the *Arabidopsis* adult leaf transcriptome. Future work will be focused on directly demonstrating that m^6A sites of specific loci inhibit ribonucleolytic cleavage when methylated and a non-methylatable mutant version of the transcript cannot be stabilized due to the absence of methylation. Additionally, identifying the ribonuclease cleaving these mRNA regions in the absence and/or following removal of m^6A at these sites is an important future direction.

Due to increasing global population, the agriculture industry must dramatically increase food production over the next 25 years. A major challenge to this problem is overcoming abiotic stresses, which limit crop survival and yield. Thus, it is essential to study plant response to abiotic stress to allow engineering of crop plants to withstand and produce normal yields under these adverse conditions. Here, we demonstrate that m^6A is dynamically deposited on transcripts encoding proteins required for proper plant salt and osmotic responses upon exposure to salt treatment in *Arabidopsis*. The addition of m^6A onto these populations of mRNAs during response to salt stress results in overall increases in stability and thereby abundance by decreasing their normally higher cleavage levels (Figures 4 and S5B). Although further studies are needed, we hypothesize that this stabilization allows the transcripts to be translated into proteins that function in salt stress response to promote adaptation to high salt levels (Figure 5C). Studies are also needed to examine whether this mechanism is shared among important crop species. In conclusion, the m^6A-mediated regulatory process we describe provides a powerful post-transcriptional mechanism for regulating transcript abundance under normal and stress conditions in eukaryotic transcriptomes and provides a means to dynamically shift stability onto populations of transcripts needed for immediate responses to environmental insults.

STAR★METHODS

Detailed methods are provided in the online version of this paper and include the following:

- KEY RESOURCES TABLE
- CONTACT FOR REAGENT AND RESOURCE SHARING
- EXPERIMENTAL MODEL AND SUBJECT DETAILS
  - Plant Materials
- METHOD DETAILS
  - RNA isolation
  - PolyA$^+$ mRNA selection
  - m^6A-seq
  - RNA sequencing
  - Genome-wide mapping of uncapped and cleaved transcripts (GMUCT)
  - Transcript stability time course
- QUANTIFICATION AND STATISTICAL ANALYSIS
  - m^6A peak calling
  - Read processing and alignment
  - Differential abundance analysis
  - Generation of random unmodified control sites
  - Highly cleaved site analysis
  - Statistical testing of motif enrichments

SUPPLEMENTAL INFORMATION

Supplemental Information includes five figures and five tables and can be found with this article online at https://doi.org/10.1016/j.celrep.2018.10.020.

ACKNOWLEDGMENTS

The authors would like to thank Dr. Gordon G. Simpson and members of the B.D.G. lab both past and present for helpful discussions as well as Dr. Paul Schmidt for use of lab resources. This work was funded by NSF grants MCB-1623887 and IOS-1444490 to B.D.G.

AUTHOR CONTRIBUTIONS

B.D.G. conceived the study. S.J.A., R.G.F., M.A.B., and B.D.G. designed the experiments. S.J.A., M.C.K., S.J.G., X.Y., L.E.V., A.D.L.N., Z.D.A., M.A.B., and B.D.G. performed experiments. S.J.A., M.C.K., X.Y., S.J.G., Z.D.A., E.L., and B.D.G. analyzed the data. S.J.A., M.C.K., and B.D.G. wrote the paper with assistance from all authors. The authors have read and approved the manuscript for publication.

DECLARATION OF INTERESTS

The authors declare no competing interests.

Received: January 29, 2018
Revised: September 4, 2018
Accepted: October 3, 2018
Published: October 30, 2018

REFERENCES

Anders, S., Pyl, P.T., and Huber, W. (2015). HTSeq–a Python framework to work with high-throughput sequencing data. Bioinformatics *31*, 166–169.

Bailey, T.L., Boden, M., Buske, F.A., Frith, M., Grant, C.E., Clementi, L., Ren, J., Li, W.W., and Noble, W.S. (2009). MEME SUITE: tools for motif discovery and searching. Nucleic Acids Res. *37*, W202–W208.

Batista, P.J., Molinie, B., Wang, J., Qu, K., Zhang, J., Li, L., Bouley, D.M., Lujan, E., Haddad, B., Daneshvar, K., et al. (2014). m(6)A RNA modification controls cell fate transition in mammalian embryonic stem cells. Cell Stem Cell *15*, 707–719.

Bodi, Z., Zhong, S., Mehra, S., Song, J., Graham, N., Li, H., May, S., and Fray, R.G. (2012). Adenosine methylation in Arabidopsis mRNA is associated with the 3′ end and reduced levels cause developmental defects. Front. Plant Sci. *3*, 48.

Deal, R.B., Henikoff, J.G., and Henikoff, S. (2010). Genome-wide kinetics of nucleosome turnover determined by metabolic labeling of histones. Science *328*, 1161–1164.

Dobin, A., Davis, C.A., Schlesinger, F., Drenkow, J., Zaleski, C., Jha, S., Batut, P., Chaisson, M., and Gingeras, T.R. (2013). STAR: ultrafast universal RNA-seq aligner. Bioinformatics *29*, 15–21.

Dominissini, D., Moshitch-Moshkovitz, S., Schwartz, S., Salmon-Divon, M., Ungar, L., Osenberg, S., Cesarkas, K., Jacob-Hirsch, J., Amariglio, N., Kupiec, M., et al. (2012). Topology of the human and mouse m^6A RNA methylomes revealed by m^6A-seq. Nature *485*, 201–206.

Duan, H.-C., Wei, L.-H., Zhang, C., Wang, Y., Chen, L., Lu, Z., Chen, P.R., He, C., and Jia, G. (2017). ALKBH10B is an RNA N6-methyladenosine demethylase affecting Arabidopsis floral transition. Plant Cell, tpc.00912.2016.

Gregory, B.D., O'Malley, R.C., Lister, R., Urich, M.A., Tonti-Filippini, J., Chen, H., Millar, A.H., and Ecker, J.R. (2008). A link between RNA metabolism and silencing affecting Arabidopsis development. Dev. Cell *14*, 854–866.

Heinz, S., Benner, C., Spann, N., Bertolino, E., Lin, Y.C., Laslo, P., Cheng, J.X., Murre, C., Singh, H., and Glass, C.K. (2010). Simple combinations of lineage-determining transcription factors prime cis-regulatory elements required for macrophage and B cell identities. Mol. Cell *38*, 576–589.

Hoagland, D.R., and Arnon, D.I. (1950). The Water-Culture Method for Growing Plants without Soil (Berkeley: University of California).

Huang, W., Sherman, B.T., and Lempicki, R.A. (2009). Systematic and integrative analysis of large gene lists using DAVID bioinformatics resources. Nat. Protoc. *4*, 44–57.

Kramer, M.C., Anderson, S.J., and Gregory, B.D. (2018). The nucleotides they are a-changin': function of RNA binding proteins in post-transcriptional messenger RNA editing and modification in Arabidopsis. Curr. Opin. Plant Biol. *45* (*Pt A*), 88–95.

Lence, T., Akhtar, J., Bayer, M., Schmid, K., Spindler, L., Ho, C.H., Kreim, N., Andrade-Navarro, M.A., Poeck, B., Helm, M., and Roignant, J.Y. (2016). m^6A modulates neuronal functions and sex determination in Drosophila. Nature *540*, 242–247.

Li, H., Handsaker, B., Wysoker, A., Fennell, T., Ruan, J., Homer, N., Marth, G., Abecasis, G., and Durbin, R.; 1000 Genome Project Data Processing Subgroup (2009). The Sequence Alignment/Map format and SAMtools. Bioinformatics *25*, 2078–2079.

Linder, B., Grozhik, A.V., Olarerin-George, A.O., Meydan, C., Mason, C.E., and Jaffrey, S.R. (2015). Single-nucleotide-resolution mapping of m6A and m6Am throughout the transcriptome. Nat. Methods *12*, 767–772.

Liu, N., Dai, Q., Zheng, G., He, C., Parisien, M., and Pan, T. (2015). $N(^6)$-methyladenosine-dependent RNA structural switches regulate RNA-protein interactions. Nature *518*, 560–564.

Love, M.I., Huber, W., and Anders, S. (2014). Moderated estimation of fold change and dispersion for RNA-seq data with DESeq2. Genome Biol. *15*, 550.

Luo, G.-Z., MacQueen, A., Zheng, G., Duan, H., Dore, L.C., Lu, Z., Liu, J., Chen, K., Jia, G., Bergelson, J., and He, C. (2014). Unique features of the m6A methylome in Arabidopsis thaliana. Nat. Commun. *5*, 5630.

Lyons, E., and Freeling, M. (2008). How to usefully compare homologous plant genes and chromosomes as DNA sequences. Plant J. *53*, 661–673.

Martin, M. (2011). Cutadapt removes adapter sequences from high-throughput sequencing reads. EMBnet.journal *17*, 10–12.

Martínez-Pérez, M., Aparicio, F., López-Gresa, M.P., Bellés, J.M., Sánchez-Navarro, J.A., and Pallás, V. (2017). *Arabidopsis* m^6A demethylase activity modulates viral infection of a plant virus and the m^6A abundance in its genomic RNAs. Proc. Natl. Acad. Sci. USA *114*, 10755–10760.

Meyer, K.D., Saletore, Y., Zumbo, P., Elemento, O., Mason, C.E., and Jaffrey, S.R. (2012). Comprehensive analysis of mRNA methylation reveals enrichment in 3′ UTRs and near stop codons. Cell *149*, 1635–1646.

Niu, Y., Zhao, X., Wu, Y.-S., Li, M.-M., Wang, X.-J., and Yang, Y.-G. (2013). N6-methyl-adenosine (m6A) in RNA: an old modification with a novel epigenetic function. Genomics Proteomics Bioinformatics *11*, 8–17.

Quinlan, A.R., and Hall, I.M. (2010). BEDTools: a flexible suite of utilities for comparing genomic features. Bioinformatics *26*, 841–842.

Shen, L., Liang, Z., Gu, X., Chen, Y., Teo, Z.W.N., Hou, X., Cai, W.M., Dedon, P.C., Liu, L., and Yu, H. (2016). N(6)-methyladenosine RNA modification regulates shoot stem cell fate in Arabidopsis. Dev. Cell *38*, 186–200.

Silverman, I.M., Li, F., Alexander, A., Goff, L., Trapnell, C., Rinn, J.L., and Gregory, B.D. (2014). RNase-mediated protein footprint sequencing reveals protein-binding sites throughout the human transcriptome. Genome Biol. *15*, R3.

Souret, F.F., Kastenmayer, J.P., and Green, P.J. (2004). AtXRN4 degrades mRNA in Arabidopsis and its substrates include selected miRNA targets. Mol. Cell *15*, 173–183.

Please cite this article in press as: Anderson et al., N^6-Methyladenosine Inhibits Local Ribonucleolytic Cleavage to Stabilize mRNAs in *Arabidopsis*, Cell Reports (2018), https://doi.org/10.1016/j.celrep.2018.10.020

Vandivier, L.E., Campos, R., Kuksa, P.P., Silverman, I.M., Wang, L.-S., and Gregory, B.D. (2015). Chemical modifications mark alternatively spliced and uncapped messenger RNAs in Arabidopsis. Plant Cell, tpc.15.00591.

Wang, X., Lu, Z., Gomez, A., Hon, G.C., Yue, Y., Han, D., Fu, Y., Parisien, M., Dai, Q., Jia, G., et al. (2014a). N^6-methyladenosine-dependent regulation of messenger RNA stability. Nature *505*, 117–120.

Wang, Y., Li, Y., Toth, J.I., Petroski, M.D., Zhang, Z., and Zhao, J.C. (2014b). N6-methyladenosine modification destabilizes developmental regulators in embryonic stem cells. Nat. Cell Biol. *16*, 191–198.

Wei, L.-H., Song, P., Wang, Y., Lu, Z., Tang, Q., Yu, Q., Xiao, Y., Zhang, X., Duan, H.-C., and Jia, G. (2018). The m6A reader ECT2 controls trichome morphology by affecting mRNA stability in Arabidopsis. Plant Cell, tpc.00934.2017.

Weyn-Vanhentenryck, S.M., Mele, A., Yan, Q., Sun, S., Farny, N., Zhang, Z., Xue, C., Herre, M., Silver, P.A., Zhang, M.Q., et al. (2014). HITS-CLIP and integrative modeling define the Rbfox splicing-regulatory network linked to brain development and autism. Cell Rep. *6*, 1139–1152.

Willmann, M.R., Berkowitz, N.D., and Gregory, B.D. (2014). Improved genome-wide mapping of uncapped and cleaved transcripts in eukaryotes–GMUCT 2.0. Methods *67*, 64–73.

Zhang, Y., Liu, T., Meyer, C.A., Eeckhoute, J., Johnson, D.S., Bernstein, B.E., Nusbaum, C., Myers, R.M., Brown, M., Li, W., and Liu, X.S. (2008). Model-based analysis of ChIP-seq (MACS). Genome Biol. *9*, R137.

Zhao, B.S., Wang, X., Beadell, A.V., Lu, Z., Shi, H., Kuuspalu, A., Ho, R.K., and He, C. (2017). m^6A-dependent maternal mRNA clearance facilitates zebrafish maternal-to-zygotic transition. Nature *542*, 475–478.

Zhong, S., Li, H., Bodi, Z., Button, J., Vespa, L., Herzog, M., and Fray, R.G. (2008). MTA is an Arabidopsis messenger RNA adenosine methylase and interacts with a homolog of a sex-specific splicing factor. Plant Cell *20*, 1278–1288.

Q2 Q3 STAR★METHODS

KEY RESOURCES TABLE

REAGENT or RESOURCE	SOURCE	IDENTIFIER
Antibodies	Source	Identifier
α-m^6A	Synaptic Systems	202-003
Chemicals, Peptides, and Recombinant Proteins		
Hoaglands Solution with or without 50 mM or 100 mM NaCl	Hoagland and Arnon, 1950	NA
Actinomycin D	Research Products International	A10025-0.005
Cordycepin	Sigma	C3394
Deposited Data		
Raw and processed m^6A IP sequencing (m^6A-seq) data	This paper	GEO: GSE108852
Raw and processed $polyA^+$-selected RNA sequencing (mRNA-seq) data	This paper	GEO: GSE108852
Raw and processed GMUCT data	This paper	GEO: GSE108852
Genome-browser view of these data	This paper	EPIC-CoGe: https://genomevolution.org/coge/NotebookView.pl?nid=2228
TAIR10 *Arabidopsis* annotation	TAIR	ftp://ftp.arabidopsis.org/home/tair/Genes/TAIR10_genome_release/
Experimental Models: Organisms/Strains		
Arabidopsis thaliana: Col-0	ABRC	CS70000
Arabidopsis thaliana: ABI3p:MTA *mta*	Bodi et al., 2012	N/A
Arabidopsis thaliana: UBQ10:NTF/ACT2p:BirA Columbia-0 (Col-0) ecotype	Deal et al., 2010	N/A
Software and Algorithms		
STAR v2.4.0	Dobin et al., 2013	https://github.com/alexdobin/STAR
Samtools v0.1.19	Li et al., 2009	https://github.com/samtools/samtools
Bedtools v2.26.0	Quinlan and Hall, 2010	https://github.com/arq5x/bedtools2
MACS2 v2.1.1.20160309	Zhang et al., 2008	https://github.com/taoliu/MACS
DEseq2 1.18.1	Love et al., 2014	https://bioconductor.org/biocLite.R
HTseq v0.6.0	Anders et al., 2015	https://github.com/simon-anders/htseq
MEME v4.11.1	Bailey et al., 2009	https://github.com/cinquin/MEME
HOMER2	Heinz et al., 2010	http://homer.ucsd.edu/homer/download.html
Cutadapt v1.9.1	Martin, 2011	https://github.com/marcelm/cutadapt/
Oligonucleotides		
RT-qPCR primers	Table S5; this study	N/A
Other		
MS Salts	Phytotech	M524

CONTACT FOR REAGENT AND RESOURCE SHARING

Further information and requests for resources and reagents should be directed to and will be fulfilled by the Lead Contact, Dr. Brian D. Gregory (bdgregor@sas.upenn.edu).

EXPERIMENTAL MODEL AND SUBJECT DETAILS

Plant Materials

All plants were grown in controlled chambers with a cycle of 16 hours light and 8 hours dark at 20°C. All experiments were performed using leaves 5-9 collected within the same 2 hour circadian window between four and six hours after first light from all plant genotypes

Please cite this article in press as: Anderson et al., N^6-Methyladenosine Inhibits Local Ribonucleolytic Cleavage to Stabilize mRNAs in *Arabidopsis*, Cell Reports (2018), https://doi.org/10.1016/j.celrep.2018.10.020

used in this study (see KRT for details)). Since MTA is expressed under an embryonic promoter, leaves 5-9 were chosen as they are far enough past embryonic development that they should lack most m^6A.

For salt stress experiments, plants were grown on soil without fertilizer and instead were initially watered with 0.25X Hoagland's solution (Hoagland and Arnon, 1950). Plants were watered with Hoagland's solution for 2 weeks before control and salt treatments began. After two weeks of growth under normal watering conditions, salt-treated plants were first watered with Hoagland's solution with added 50 mM NaCl. Three days later, they were watered again with Hoagland's with added 100 mM NaCl. The flats were then watered with 150 mM NaCl Hoagland's solution every three days for a total of four additional treatments. Control flats were watered at the same time as salt-treated plants, with solely Hoagland's solution. After treatments, rosette leaves were collected from control and salt-treated flats and immediately flash frozen in liquid nitrogen.

METHOD DETAILS

RNA isolation

All experiments described in this study were performed with RNA extracted from leaves 5-9 homogenized using a liquid N_2 cooled mortar and pestle. RNA was extracted from homogenate using Qiazol lysis reagent, and further homogenized using Qiashredders (QIAGEN, Valencia, CA, USA). RNA was then isolated using QIAGEN miRNEasy mini columns (QIAGEN, Valencia, CA, USA), as described in the included protocol. For RNA extractions from control and salt treated leaves, tissue was ground in liquid N_2, added to Qiazol lysis reagent and homogenized using an OMNI tissue homogenizer (OMNI International, Kennesaw, GA, USA). RNA was then isolated as described above. All RNA was then treated with RNase-free DNase (QIAGEN, Valencia, CA, USA) at RT for 30 minutes and ethanol precipitated.

PolyA$^+$ mRNA selection

Two rounds of polyA$^+$ selection were performed using Dynabeads oligo DT bound beads from the Dynabeads mRNA direct purification kit (61011, ThermoFisher, Waltham, MA, USA). This process was performed as described in the Dynabeads mRNA direct purification kit for the RNA samples used for RNA-seq, GMUCT, and m^6A-seq.

m^6A-seq

m^6A-seq was performed using 7 μg of polyA$^+$ selected mRNA per replicate (Col-0 and *mta*) or 3 μg of polyA$^+$ selected mRNA per replicate (control and salt stress treated leaves). Samples were placed at 75°C for 5 minutes and then snap cooled on ice for 2 minutes. Samples were brought to 686 μL with nuclease free water. Next, 10 μL RNaseOUT (Life Technologies; Carlsbad, CA, USA), 200 μL 5X IP buffer (250 mM tris HCl, 750 mM NaCl, 0.5% vol/vol Igepal[CA-6300]), and 3 μL of m^6A antibody (ab151230, Abcam, Cambridge, UK) were added to samples which were rotated at 4°C for 2 hours. While rotating, Protein A bead slurry was washed twice with 1 mL 1X IP buffer and resuspended in 1 mL 1X IP buffer, which was supplemented with 0.5 mg/mL BSA and rotated for 2 hours at 4°C. After 2 hours, the RNA samples were transferred into 3 cm cell culture dishes and cross-linked twice with 0.15 J/cm^2 UV light in an Agilent Stratalinker. Protein A beads were then pelleted using a magnetic strand and washed twice using 1 mL 1X IP buffer. 250 μL of bead mixture and RNA samples were placed into a 2 mL tube and rotated for 2 hours at 4°C. After 2 hours, beads were pelleted using a magnetic stand, supernatant was removed, and stored at −80°C as unbound supernatant. Bead bound samples were removed from beads by adding 95 μL proteinase K buffer, 5 μL of proteinase K, and treated for 45 minutes at 50°C, agitating every ten minutes. Supernatant was removed and stored at −80°C as the m^6A+ sample. Beads were washed twice using 300 μL 1X IP buffer. Supernatant from both washes were also stored as m^6A+ samples. All samples were precipitated using glycogen, NaOAc and 3X vol/vol 100% ethanol and kept at −80°C overnight. m^6A+ samples were then pooled after resuspension in nuclease free water. m^6A+ and the unbound supernatant samples were then prepared into libraries using a strand-specific RNA sequencing library preparation protocol as previously described (Silverman et al., 2014).

RNA sequencing

RNA sequencing (RNA-seq) of RNA samples from 4-week-old Col-0 and *mta* leaves was performed using the Illumina TruSeq Stranded mRNA kit (20020594, Illumina, San Diego, CA, USA) as described in the manual supplied with the kit. For control and salt stressed RNA-seq, polyA$^+$ RNA was first isolated as described above before library preparation was performed as previously described (Silverman et al., 2014).

Genome-wide mapping of uncapped and cleaved transcripts (GMUCT)

GMUCT libraries were constructed and sequenced for all samples used in this study as previously described (Willmann et al., 2014).

Transcript stability time course

5-day-old seedlings (10 individuals per replicate) grown on 0.5X MS agar plates were carefully transferred into 0.5X MS liquid growth media containing 10 μM Actinomycin D and 0.6 mM cordycepin. Plants were then harvested at 0 and 24 hours post-treatment. Total RNA was extracted and reverse transcribed using oligo dT primers. Quantification of gene levels at 0 and 24 hours was performed using qRT-PCR (Table S5).

QUANTIFICATION AND STATISTICAL ANALYSIS

m^{6}A peak calling

To identify regions in which m^{6}A modifications occurred we used the peak calling algorithm MACS2 on input files that had been separated into reads that mapped to the positive and negative strand respectively. The MACS2 callpeak function was run with the following parameters:–nomodel,–extsize 50, -p 5e-2, and –g 32542107. The –g option accounts for one-half the size of the *Arabidopsis* transcriptome as input files were exclusively + or – stranded. As a background for MACS2, we used our m^{6}A- (m^{6}A supernatant) samples, thus peaks were identified as enriched upon pull down with the m^{6}A antibody compared to background.

Read processing and alignment

Reads from all high-throughput RNA sequencing approaches were trimmed to remove 3′ sequencing adapters with Cutadapt (version 1.2.1 using parameters -e 0.06 -O 6 -m 14). The resulting trimmed sequences were aligned to the TAIR10 *Arabidopsis* genome sequence using STAR (version 2.4.0 with parameters–clip3pAdapterSeeq TGGAATTCTCGGGTGCCAAGG and for m^{6}A-seq libraries the parameter –bamRemoveDuplicatesType UniqueIdentical).

Differential abundance analysis

Gene counts for each transcript were called using HTseq-count on aligned RNA-seq reads using the parameters–format = bam–stranded = reverse–mode = intersection-strict. Differentially abundant genes were called using the R package DESeq2 (Love et al., 2014) on all replicates of *mta* and Col-0 using default parameters. Validaiton of the differential transcript abundances was done using qRT-PCR (Table S5).

Generation of random unmodified control sites

We generated control sites that lacked m^{6}A modifications by using the bedtools function shuffleBed. Parameter –i was used to shuffle m^{6}A peaks into random sites, parameter -incl was used to constrain shuffling to regions that were at or 3′ of 50 nt upstream of stop codons in unmodified transcripts.

Highly cleaved site analysis

To identify highly cleaved sites within m^{6}A peaks, we calculated the read coverage of only the 5′ ends of GMUCT reads within each m^{6}A peak and defined the position with the highest 5′ end read coverage as the most cleaved.

Statistical testing of motif enrichments

Testing for enrichment of a particular motif within a window was performed using the motif enrichment analysis algorithm Homer2 known (Heinz et al., 2010).

Statistical testing of interactions

Analysis of 2-way interactions was performed using a hypergeometric enrichment analysis with total population defined as all genes that appear in either genotype. In order to test 3-way interactions a 2x2x2 Log-linear analysis was used.

Identification of cross-linking induced mutation sites (CIMS)

To do this, we trimmed adapters from m^{6}A+ library fastq files using cutadapt and subsequently converted these files to fasta format. PCR duplicates were collapsed and aligned using Novalign with parameters -l 15 -s 1. Mismatch files were generated using novoalign2bed.pl with parameters -v –mismatch-file as previously described (Weyn-Vanhentenryck et al., 2014). Peaks were called with respect to strand using tag2profile with parameters -v -ss -exact. Mutations were extracted to unique CIMS tags using the tool joinWrapper. CIMS were then filtered into candidate A or C's that were mutated and that had a frequency score of > 30.

DATA AND SOFTWARE AVAILABILITY

Accession numbers

The raw and processed data for m^{6}A-seq, RNA-seq, and GMUCT from our analyses of both Col-0 and *mta* adult leaves as well as control and salt stressed tissue have been deposited into the NCBI Gene Expression Omnibus (GEO) database under the accession number GSE108852.

Genome browser availability

The sequencing data presented here is also available through the EPIC-CoGe genome browser (Lyons and Freeling, 2008): https://genomevolution.org/coge/NotebookView.pl?nid=2228.

Cell Reports, Volume *25*

Supplemental Information

N^6-Methyladenosine Inhibits Local Ribonucleolytic Cleavage to Stabilize mRNAs in *Arabidopsis*

Stephen J. Anderson, Marianne C. Kramer, Sager J. Gosai, Xiang Yu, Lee E. Vandivier, Andrew D.L. Nelson, Zachary D. Anderson, Mark A. Beilstein, Rupert G. Fray, Eric Lyons, and Brian D. Gregory

N^6-methyladenosine inhibits local ribonucleolytic cleavage to stabilize messenger RNAs in *Arabidopsis*

Stephen J. Anderson, Marianne C. Kramer, Sager J. Gosai, Xiang Yu, Lee E. Vandivier, Andrew D.L. Nelson, Zachary D. Anderson, Mark A. Beilstein, Rupert G. Fray, Eric Lyons, and Brian D. Gregory

SUPPLEMENTAL FIGURES

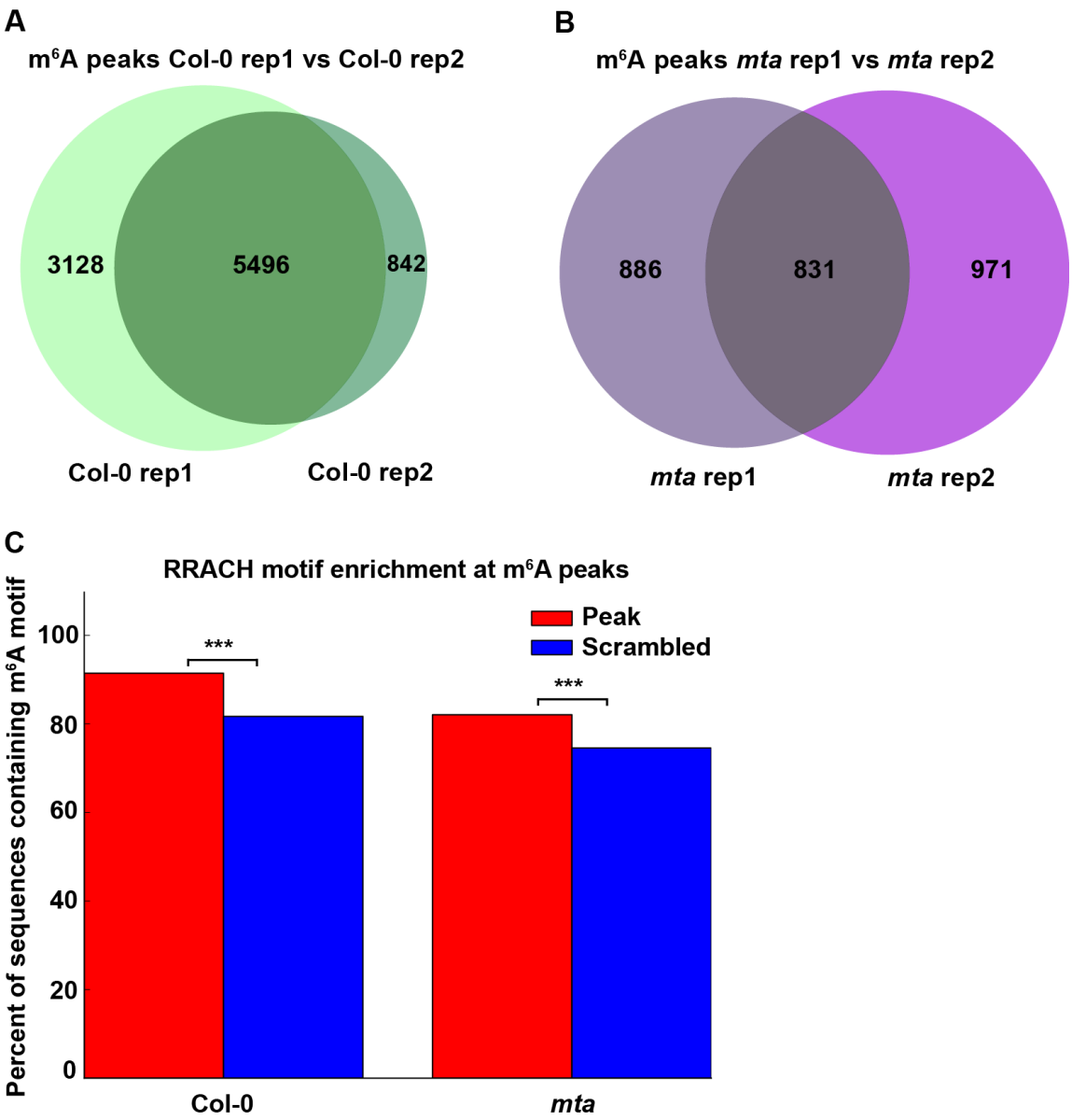

Figure S1: m^{6}A-seq identifies bona fide m^{6}A peaks in the *Arabidopsis* adult leaf transcriptome, Related to Figure 1.

(A-B) Overlap between m^{6}A peaks identified in two biological replicate experiments using leaves 5-9 from 4-week-old Col-0 (A) and *mta* (B) plants. Only peaks found in both replicates for each genotype were used for subsequent analyses. (C) Enrichment of the canonical m^{6}A motif (RRACH) in Col-0 and *mta* m^{6}A peaks as compared to scrambled controls. *** denotes *p* value < 0.001, chi-squared test.

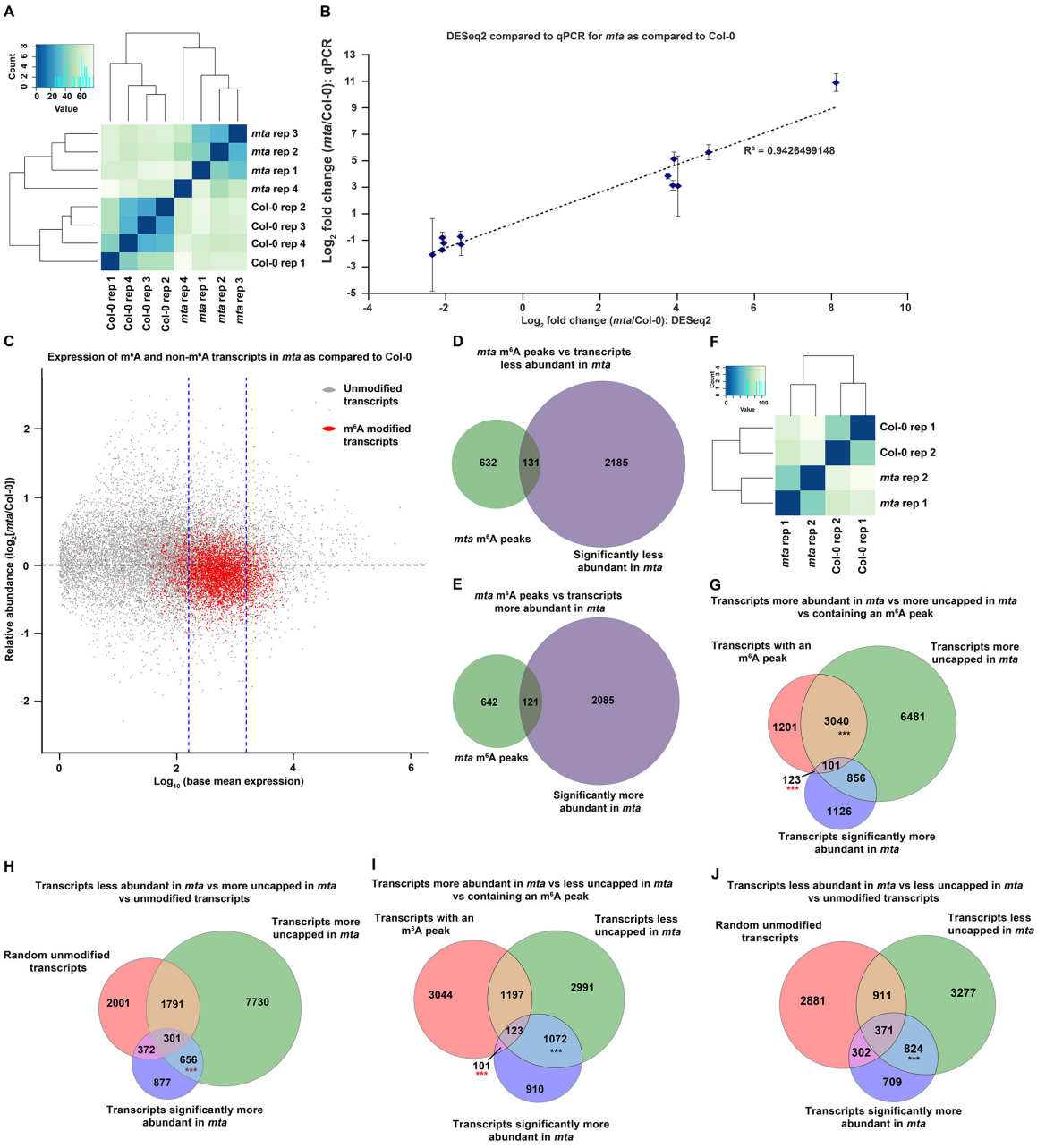

Figure S2: Comprehensive RNA-seq and genome-wide mapping of uncapped and cleaved transcripts (GMUCT) analyses of the Col-0 and *mta* transcriptomes reveal that 3' localized m^{6}A is a stabilizing mark in the *Arabidopsis* adult leaf transcriptome, Related to Figure 2.

(A) Clustering analysis of the 4 mRNA-seq biological replicates for 4-week-old Col-0 and *mta* leaves (8 total libraries). HTSeq was used to count the number of reads mapping to each gene in the TAIR10 transcriptome. Based on these HTSeq read counts from Col-0 and *mta* mRNA-seq replicates, the libraries were

clustered based on a correlation analysis via DESeq2 (Love et al., 2014). This analysis revealed high levels of similarity within libraries corresponding to the biological replicates, as each genotype clustered together. (B) The mRNA abundance fold change values for *mta* relative to Col-0 leaf transcriptomes as calculated by DESeq2 analysis (x-axis) and qPCR (y-axis) for a number of transcripts selected for validation. The strong correlation ($R^2 > 0.94$) between these values demonstrates the validity of the DESeq2 findings. (C) The overall abundance of transcripts in Col-0 (x-axis) and the relative abundance of transcripts in *mta* as compared to Col-0 (y-axis) calculated using DESeq2 (Love et al., 2014). Red dots denote high-confidence m^6A modified transcripts, while gray dots denote transcripts that do not contain a high-confidence m^6A peak. Vertical blue dotted lines represent the expression bounds for m^6A transcripts used in calculating the proportion uncapped metric (see Figure 3A). (D-E) The overlap between high-confidence *mta* m^6A peaks and transcripts significantly less (D) and more (E) abundant in *mta* plants. F) Clustering analysis of all four genome-wide mapping of uncapped and cleaved transcripts (GMUCT) libraries. HTSeq was used to count the number of reads mapping to each gene in the TAIR10 transcriptome. Based on these HTSeq read counts from Col-0 and *mta* GMUCT replicates, the libraries were clustered based on a correlation analysis via DESeq2 (Love et al., 2014). This analysis revealed high levels of similarity within libraries corresponding to the biological replicates, as each genotype clustered together. (G-J) Venn diagrams showing overlap between various groups of transcripts as specified in each figure. *** denotes a significant (*p* value < 0.001) overlap between the specified transcript populations, log-linear analysis. *** denotes *p* value < 0.001 for less than expected in the overlap, log-linear analysis.

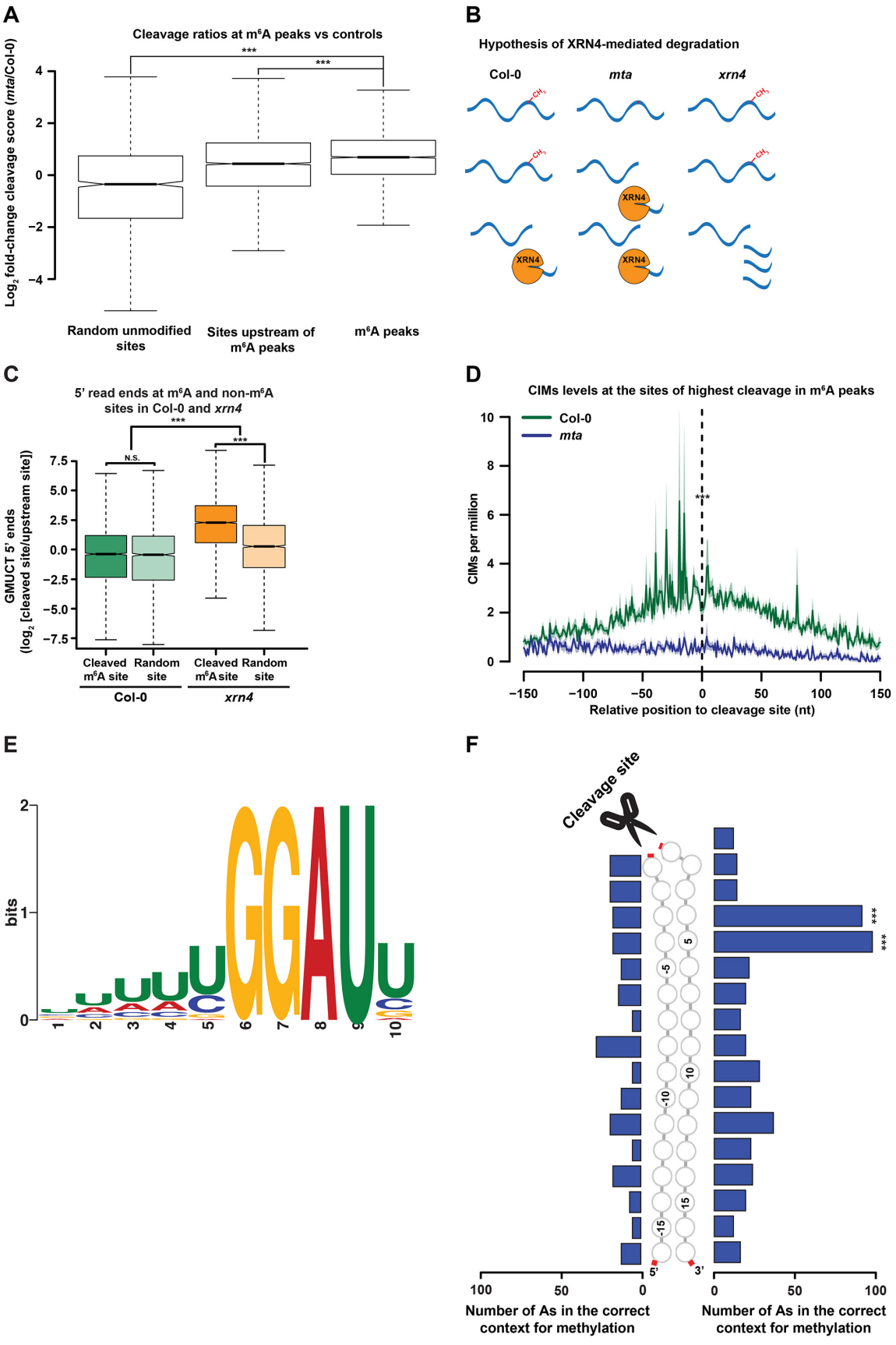
A
Cleavage ratios at m6A peaks vs controls
***
***
Log2 fold-change cleavage score (mta/Col-0)
4
2
0
−2
−4
Random unmodified sites
Sites upstream of m6A peaks
m6A peaks
B
Hypothesis of XRN4-mediated degradation
Col-0
mta
xrn4
CH3
XRN4
C
5' read ends at m6A and non-m6A sites in Col-0 and xrn4
***
***
N.S.
GMUCT 5' ends (log2 [cleaved site/upstream site])
7.5
5.0
2.5
0.0
−2.5
−5.0
−7.5
Cleaved m6A site
Random site
Cleaved m6A site
Random site
Col-0
xrn4
D
CIMs levels at the sites of highest cleavage in m6A peaks
Col-0
mta
CIMs per million
10
8
6
4
2
0
***
−150
−100
−50
0
50
100
150
Relative position to cleavage site (nt)
E
bits
2
1
0
1
2
3
4
5
6
7
8
9
10
F
Cleavage site
5'
3'
5
-5
10
-10
15
-15
***
***
100
50
0
Number of As in the correct context for methylation
0
50
100
Number of As in the correct context for methylation

Figure S3: m^{6}A modification on canonical and non-canonical motifs in protein-coding mRNAs inhibits local ribonucleolytic cleavage, Related to Figure 3.

(A) The $\log_2$ *mta*/Col-0 cleavage score ratio for m^{6}A peaks as compared to same sized windows 300 nt upstream of these peaks as well as compared to randomly selected sites towards the 3' end of unmodified transcripts. *** denotes *p* value < 0.001, Wilcoxon ranked sum test. (B) Hypothesis of XRN4-mediated degradation of downstream (3') cleavage products. (C) Change in accumulation of GMUCT 5' read ends +/- 25 nt up- and downstream of m^{6}A-regulated cleavage sites compared to +/- 25 nt up- and downstream of the nucleotide 300 nt upstream of those sites (cleaved site/upstream site) for m^{6}A-regulated cleavage sites (darker colored boxes) as compared to randomly-selected unmodified control 3' UTR sites (lighter colored boxes) using data from Col-0 (green boxes) or *xrn4* mutant (orange boxes) plants. *** denotes *p* value < 0.001, Wilcoxon ranked sum test. (D) Analysis of cross-linking induced mutation sites (CIMS) (Linder et al., 2015) +/- 150 nt of highly cleaved sites in Col-0 m^{6}A peaks. The highly cleaved site is centered at 0 in this plot. This analysis suggests we are identifying bona fide m^{6}A sites that inhibit local ribonucleolytic cleavage in the 3' UTRs of specific m^{6}A-modified *Arabidopsis* adult leaf protein-coding mRNAs. (E) A motif discovered within a 15 nt window (7 nt up- and downstream) around the highest cleaved nucleotide within Col-0 m^{6}A peaks using MEME, which appears to be a new m^{6}A motif. (F) The number of A's that occur in the GG<u>A</u>U context in the immediate vicinity of the most cleaved nucleotide within Col-0 m^{6}A peaks. The scissors denote the most cleaved nucleotide within Col-0 m^{6}A peaks. Circles to the left of the scissors represent nucleotides (nt) upstream (5') of the cleavage site, while those to the right are nt downstream (3') of these sites. Only the first A found in this sequence context in both directions is counted on this graph. *** denotes nt with *p* values < 0.001, chi-squared test.

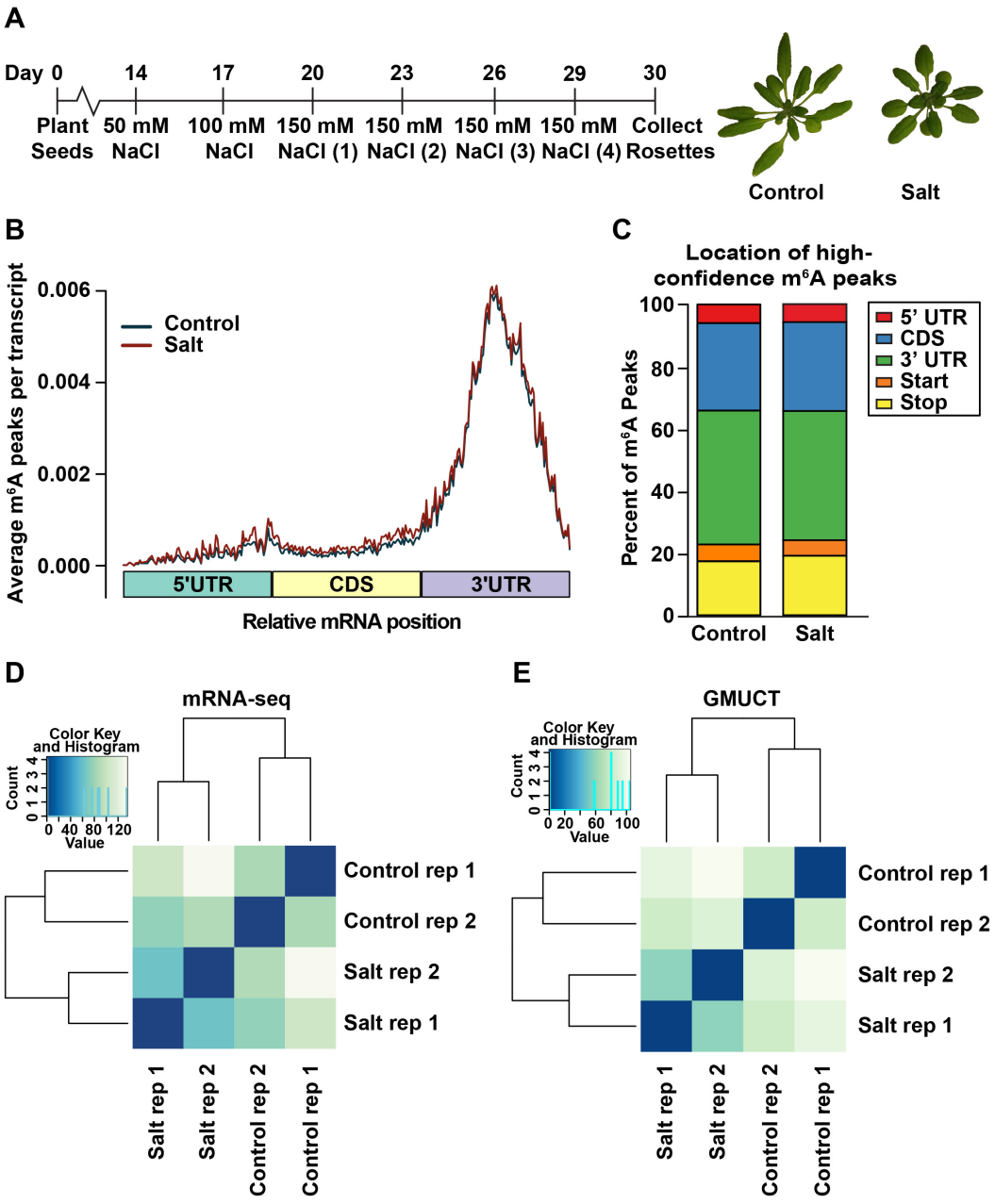

Figure S4: m^{6}A-seq identifies bona fide m^{6}A peaks in control- and salt-treated *Arabidopsis* plants, which display similar localization patterns to those observed in the 4-week-old Col-0 leaf transcriptome, Related to Figure 4.

(A) Overview of long-term, agriculturally-relevant salt stress treatments. After two weeks of growth on soil with normal watering conditions, salt-treated plants were watered every three days with increasing concentrations of NaCl in 50 mM increments until the final salt concentration of 150 mM was reached. The salt-treated plants were watered a total of three times with 150 mM NaCl. The control plants were grown and watered on the same schedule without the addition of NaCl to the wetting solution. Upon completion of treatments, the rosette leaves of salt-treated plants were much smaller and darker green when compared to control plants. These phenotypes were a result of decreased growth and increased stress pigment production in the salt-treated plants. (B) The localization pattern of control- (blue) and salt-specific (red) m^6A peaks in Arabidopsis mRNAs. (C) Percentage of total control and salt high-confidence m^6A peaks located in the specified regions of mRNA transcripts. Peaks that overlapped a start or stop codon were designated as start or stop codon peaks. (D-E) Clustering analysis of the mRNA-seq (D) and GMUCT (E) libraries for control and salt treated plants. HTSeq was used to count the number of sequencing reads mapping to each gene in the TAIR10 transcriptome. Based on these HTSeq read counts from control- and salt-treated plants, the libraries were clustered based on a correlation analysis via DESeq2 (Love et al., 2014). This analysis revealed high levels of similarity within libraries corresponding to the biological replicates, as each genotype clustered together.

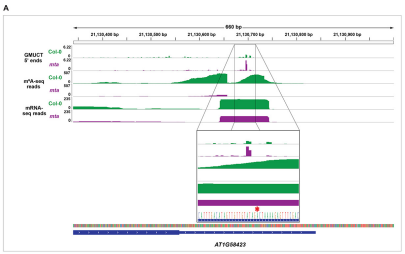
A
660 bp
GMUCT 5' ends
m⁶A-seq reads
mRNA-seq reads
Col-0
mta
AT1G08420

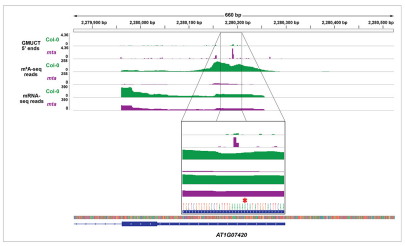
660 bp
GMUCT 5' ends
m⁶A-seq reads
mRNA-seq reads
Col-0
mta
AT1G07420

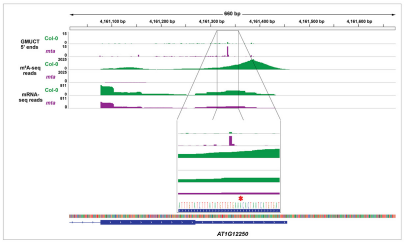
660 bp
GMUCT 5' ends
m⁶A-seq reads
mRNA-seq reads
Col-0
mta
AT1G12250

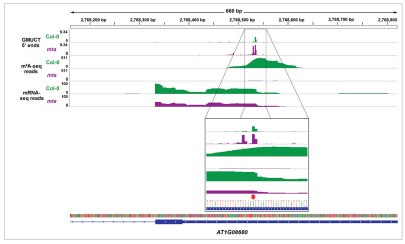
660 bp
GMUCT 5' ends
m⁶A-seq reads
mRNA-seq reads
Col-0
mta
AT1G08560

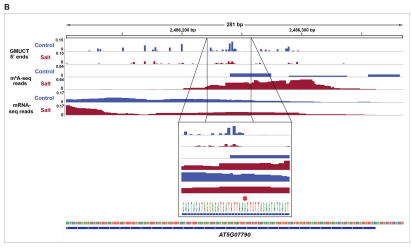
B
281 bp
GMUCT 5' ends
m⁶A-seq reads
mRNA-seq reads
Control
Salt
AT5G07790

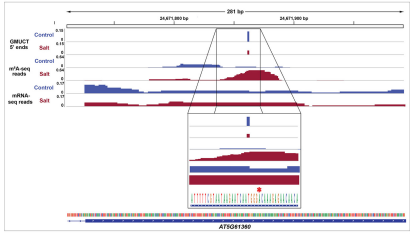
281 bp
GMUCT 5' ends
m⁶A-seq reads
mRNA-seq reads
Control
Salt
AT5G61360

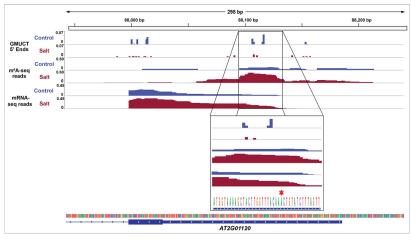
286 bp
GMUCT 5' Ends
m⁶A-seq reads
mRNA-seq reads
Control
Salt
AT2G01120

Figure S5: Browser views of m^{6}A-mediated regulation of ribonucleolytic mRNA cleavage and subsequent turnover, Related to Figures 1-5.
(A) Additional browser views of example transcripts (*AT1G56423*, *AT1G07420*, *AT1G12250*, and *AT1G08680* (from top to bottom, respectively)) demonstrating increased proportion uncapping and cleavage 4 and 5 nt upstream of RRACH motifs (red asterisks) and reduced expression in *mta* (purple tracks) as compared to Col-0 (green tracks). (B) Browser views of example transcripts (*AT5G07790*, *AT5G61360*, and *AT2G01120* (from top to bottom, respectively)) demonstrating increased cleavage 4 and 5 nt upstream of RRACH motifs (red asterisks) and reduced expression in control- (blue tracks) as compared to salt-treated (red tracks) plants.